TRPA1 mediates sensation of the rate of temperature change in Drosophila larvae

by
Junjie Luo

A dissertation submitted to Johns Hopkins University in conformity with the requirements for the degree of Doctor of Philosophy

Baltimore, Maryland

May, 2017

Abstract

Avoidance of noxious ambient heat is crucial for animal survival. An important class of molecules that contributes to thermosensation is Transient Receptor Potential channels (thermoTRPs). ThermoTRPs are activated directly or indirectly by changes in temperatures, enabling animals to respond behaviorally to temperature fluctuations in the environment. The founding thermoTRP, mouse TRPV1, is activated by temperature higher than 42°C, and is required for avoidance of noxious heat. Other mammalian thermoTRPs are activated with different thresholds, such as mouse TRPM8 and TRPA1, which are activated directly by temperatures below ~23°C and ~17°C, respectively.

The contribution of TRPs to thermosensation is evolutionarily conserved, and is well-documented in the invertebrate model organisms: *C. elegans* and *Drosophila melanogaster*. In *Drosophila* larvae, noxious heat is detected through direct activation of three TRPA channels: Painless, Pyrexia and TRPA1. The TRPA1 channel also enables larvae to sense small deviations above the preferred temperature. In the comfortable range, this fine thermal detection occurs through indirect activation of TRPA1 via a rhodopsin-dependent thermosensory signaling cascade. This signaling cascade may serve to lower the threshold for direct activation of TRPA1.

The extensive studies on thermoTRPs in model organisms have contributed greatly to the theme that warm or hot temperatures of different thresholds are sensed by direct activation of TRP channels. However, a long-known but poorly understood phenomenon is that the rate of temperature change, rather than just the

temperature threshold can affect the nociceptive response. Classic experiments on frogs performed more than 130 years ago demonstrated their high sensitivity and escape response to fast rises in heat, and indifference to slow increases in temperature. Stronger nociceptive reactions to fast temperature rises have been documented throughout the animal kingdom, in organisms as diverse as worms and humans. However, the mechanism underlying temperature rate detection is not clear.

To explore the mechanism through which an animal responds differentially to slow and fast elevations in temperature, we developed *Drosophila* larvae as an animal model. We found that if we challenged larvae with a rapid temperature rise, a very high proportion of the animals exhibited nociceptive rolling behavior. However, if the temperature increase was gradual, the percentage of larvae that rolled was much lower, even after we exceeded temperatures that induced robust nociceptive avoidance after a fast temperature increase. We found one of the TRPA1 isoforms was the key rate-sensor, and was required for neurons in the brain to respond to the rate of temperature increase, rather than just the temperature threshold. Our results indicate that larvae use a TRPA1-dependent rate-sensing mechanism to safeguard the brain from exposure to noxious heat.

Advisor: Dr. Craig Montell

Department of Biological Chemistry, Johns Hopkins University School of Medicine

Neuroscience Research Institute, University of California, Santa Barbara

MCDB Department, University of California, Santa Barbara

Reader: Dr. Xinzhong Dong

Department of Neuroscience, Johns Hopkins University School of Medicine

Howard Hughes Medical Institute, Johns Hopkins University School of Medicine

Acknowledgements

First and foremost, I want to express my sincere gratitude to my advisor Dr. Craig Montell. He provided me the chance to work in his lab and provide training on scientific research during my graduate journey. I am always inspired by his immense knowledge and enthusiasm in science. The discussions with him were full of valuable insights, fun and eye opening. I also benefited greatly from his emphasis on clear oral and written presentations, which will be important skills throughout my scientific career.

I would also like to acknowledge my thesis committee members, Dr. King-Wai Yau, Dr. Xinzhong Dong, and Dr. Christopher Potter. They paid close attention to the progress during my Ph.D. studies and provided insightful comments and encouragement. After our lab moved to the University of California, Santa Barbara, they still participated in committee meetings by Skype and continued to support my research.

My next tribute goes to Dr. Michael Caterina and Dr. Natasha Zachara, co-Directors of the Graduate Program in Biological Chemistry. They also provided guidance during my graduate studies. I appreciate their time and patience with me.

I would like to thank Dr. Wei Shen. I got to know him when we studied in the Biology Department at Tsinghua University. Fortunately, I then joined the same lab as Wei. As a senior graduate student, he provided guidance and helped me pass the most difficult period of my graduate studies. During our collaboration on the thermosensation project, I learned a lot of experimental skills from Wei. I would also like to thank my lab colleagues, Dr. Jiangqu Liu and Dr. Hsiang-Chin

Chen, for assistance in performing blind optogenetic experiments, and several undergraduate interns for assistance in generating knock-in fly lines: Madeline Macdonald, Huqiao Luo, Arian Mostofi and Keenan Chung.

Last but not least, I want to thank my family members. The great encouragement and support from my grandparents and my parents are hard to imagine. The accomplishment of my Ph.D. would not have been possible without them.

Table of Contents

List of Figures

Chapter 1

Chapter 2

Chapter 1. Introduction

Introduction

I. Temperature sensation in animals

Temperature influences the heat exchange between a living organism and the surroundings, as well as all the biochemical reactions inside the organism. Detecting temperature accurately is necessary for animals, because it enables them to maintain their homeostasis, quickly avoid noxious temperatures dangerous to their survival, or seek out their preferred temperature within their thermal landscape. Disease-transmitting insects, such as mosquitoes that spread malaria, dengue fever and yellow fever, use thermotaxis as a critical strategy to find their human hosts. Thus, chemicals that perturb this behavior may be used as insect repellents to reduce the incidence of insect-borne disease.

The famous boiling frog experiment, first performed in the 19th century, shows that animals are able to sense the rate of temperature change [1-4]. In the past century, there has been controversy over this experiment. Most of the controversy focused on whether the frog would have been boiled to death if the temperature rose slowly enough. But it is clear that the response of a frog is reduced when the temperature-changing rate is decreased [5]. This dependence of temperature sensitivity on the rate of temperature change is a common phenomenon in most animals, ranging from invertebrates to vertebrates [6].

II. TRP channels and other temperature-sensitive channels

An important class of molecules that contributes to thermotactic behavior is Transient Receptor Potential (TRP) channels [7, 8]. These proteins are critical for thermosensation in organisms ranging from worms and flies to mammals.

At the molecular level, different thermosensitive TRPs respond to distinct temperature ranges to activate neurons and other cell types. Multiple TRP channels are activated by warm or hot temperatures. These include mammalian TRPV1, which is activated by temperatures >43°C [9], and TRPV2, which is activated by temperatures >52°C [10].

In *Drosophila*, TRPA1 are expressed as multiple isoforms through alternative RNA splicing, TRPA1-A (TRPA1 isoform A) is activated with a temperature threshold of ~24–29°C [11]. The temperature threshold of TRPA1-D (TRPA1 isoform D) is higher (34°C) [12, 13]. Two other TRPA channels, Painless and Pyx are gated by noxious temperatures (>40°C) [14-16].

Several cool and cold sensitive cation channels are known. The best-characterized cold sensor in mammals is TRPM8, which is activated by cool temperatures (<30°C) [17]. Electrophysiological experiments suggest that mammalian TRPA1 is a cold sensor [18]. In *Drosophila*, there are no direct experimental results demonstrating that a channel is directly activated by cool or cold temperatures. However, TRPL and two TRPV channels, Iav and Nan, function in the behavioral aversion of larvae to cool temperatures [19, 20]. In addition, three fly TRPP-related proteins, Brv1, Brv2, and Brv3, participate in the behavioral response to low temperatures in adults [21]. *Drosophila* 3rd instar

larvae avoid temperatures in the comfortable range slightly higher than their preferred temperature (18°C) through a signaling pathway that is initiated by rhodopsins, and culminates with activation of TRPA1 [22-24]. Besides thermoTRPs, the mammalian ANO1 chloride channel, the calcium channel regulator STIM1 and *Drosophila* Gr28b-D (Gr28b isoform D) appear to function in warm sensation [25-27], while *Drosophila* IR21a, IR25a are reported to function in cool sensation [28].

Mammalian TRPA1 can be activated by cold temperatures, and is desensitized through a Ca^{2+} dependent mechanism [29, 30]. In contrast, rattlesnake TRPA1 is the opposite. It is activated by warm temperatures[31], and is not desensitized by Ca^{2+} [30]. Analyses of chimeric of human TRPA1 (hTRPA1) and rattlesnake TRPA1 (rTRPA1) indicate that the Ca^{2+}-dependent desensitization in human TRPA1 is specified by the 7^{th}~14^{th} ankyrin repeats (ARs) [30], while the heat-sensitive domains of rTRPA1 include AR 10~15 (primary module) and AR 3~8 (enhancer module) [30]. Interestingly, our data indicate that *Drosophila* TRPA1 is adaptive and its desensitization is dependent on Ca^{2+}. These findings suggest that the N-terminus of TRPA1 detects temperature and integrates temperature-changing signals into neuronal activity to control the global nociceptive response exhibited by *Drosophila* larvae.

III. The primary temperature-sensing neurons

Various neurons express thermo-sensitive molecules to sense and transmit temperature signals to guide behaviors in response to the environment. In

mammals, projections from the dorsal root ganglion (DRG) neurons are embedded in mammal skin. DRGs can be divided into several subtypes on the basis of the sensors they express, including hot nociceptors (expressing TRPV1), putative hot-cold polymodal nociceptors (expressing TRPV1 and TRPA1), high-threshold hot nociceptors (expressing TRPV2) and cold sensors (expressing TRPM8) [32, 33]. TRPV4 is expressed in the anterior hypothalamus and its temperature-activated current is similar to that of the pre-optic anterior hypothalamus (POAH) cell, which is responsible for temperature homeostasis [34-36].

Neurons that function in temperature sensation in Drosophila are have also been described. The antenna arista in adult flies include “hot cells” (expressing Gr28b-D) and “cold cells” (expressing Brv1, 2, 3), which detect high and low temperatures respectively, and project to separate “hot” and “cold” regions of the proximal-antennal-protocerebrum (PAP) in the brain [21, 25]. Anterior cell (AC) neurons in the brain express TRPA1, and also send projections to the “hot” region of the PAP [21]. Activating both of the “hot” and “cold” regions of the PAP mediate aversive responses, to enable the adult flies to select their preference temperature [21]. Hot cells can fully contact the air, and mediate rapid responses to heat. Conversely, it takes time for heat to be transmitted to AC neurons in the brain. Thus, hot cells mediate rapid warm avoidance, while direct activation of AC neurons controls slowly developing temperature preference responses of flies [25, 37].

IV. The behavioral response to rate of temperature change in *Drosophila* larvae

Here we used *Drosophila* larvae as a model to analyze how animals respond to rates of temperature changes, rather than just the absolute temperature. It is rational to use flies to study this phenomenon since most of the temperature sensing genes in mammals are conserved in flies. Therefore, flies provide a genetically tractable model organism to reveal common mechanisms of thermosensation.

Drosophila larvae avoid suboptimal temperatures by increasing their turning rate, and thereby, choose their ideal temperatures (18°C). Compared to normal wiggling, which functions in forward movement, rolling dramatically increases movement speed. Therefore, rolling behavior is used by larvae to escape from dangerous, noxious heat. Larvae show nociceptive rolling behaviors when touched by hot probe (>45°C) and this behavior is dependent on type IV multidendritic neurons expressing both Painless and TRPA1-C in the body wall [7, 14, 38, 39]. Here, we characterize a new type of nociceptive rolling behaviors triggered by heating the whole larva, which we call the "global nociception," to distinguish it from previously described "local nociception" [40]. Because global heating is more harmful than heating small parts of the body, the threshold of global nociception is lower than local nociception. The local nociceptive response depends on a combination of thermo-pain and proprioception, because the rolling direction is impacted by the direction in which the stimulus is initiated [39]. In contrast, the rolling caused by global nociception shows the same probability of

rolling to the left or right. Interestingly, we found that the temperature sensor that is required for rolling behavior (TRPA1-A) has a lower heat threshold than the other heat sensitive TRPA1 isoform, and its expression is restricted to the larva brain. Furthermore, we found that the neurons controlling global nociception and thermotaxis are distinct subsets of *trpA1-A* neurons.

Of primary importance, we found that the global rolling behavior in response to noxious heat is determined by both temperature and temperature changing rate. This feature makes *Drosophila* larvae a great model to study thermal desensitization. To investigate whether the rate of temperature change is calculated in the primary sensor or a downstream neuronal circuit, we monitored the activity of *trpA1* neurons under different temperature changing rates. Our results demonstrate that the temperature and temperature change signals are integrated by heat-sensing cells in the brain, and by desensitization of TRPA1-A.

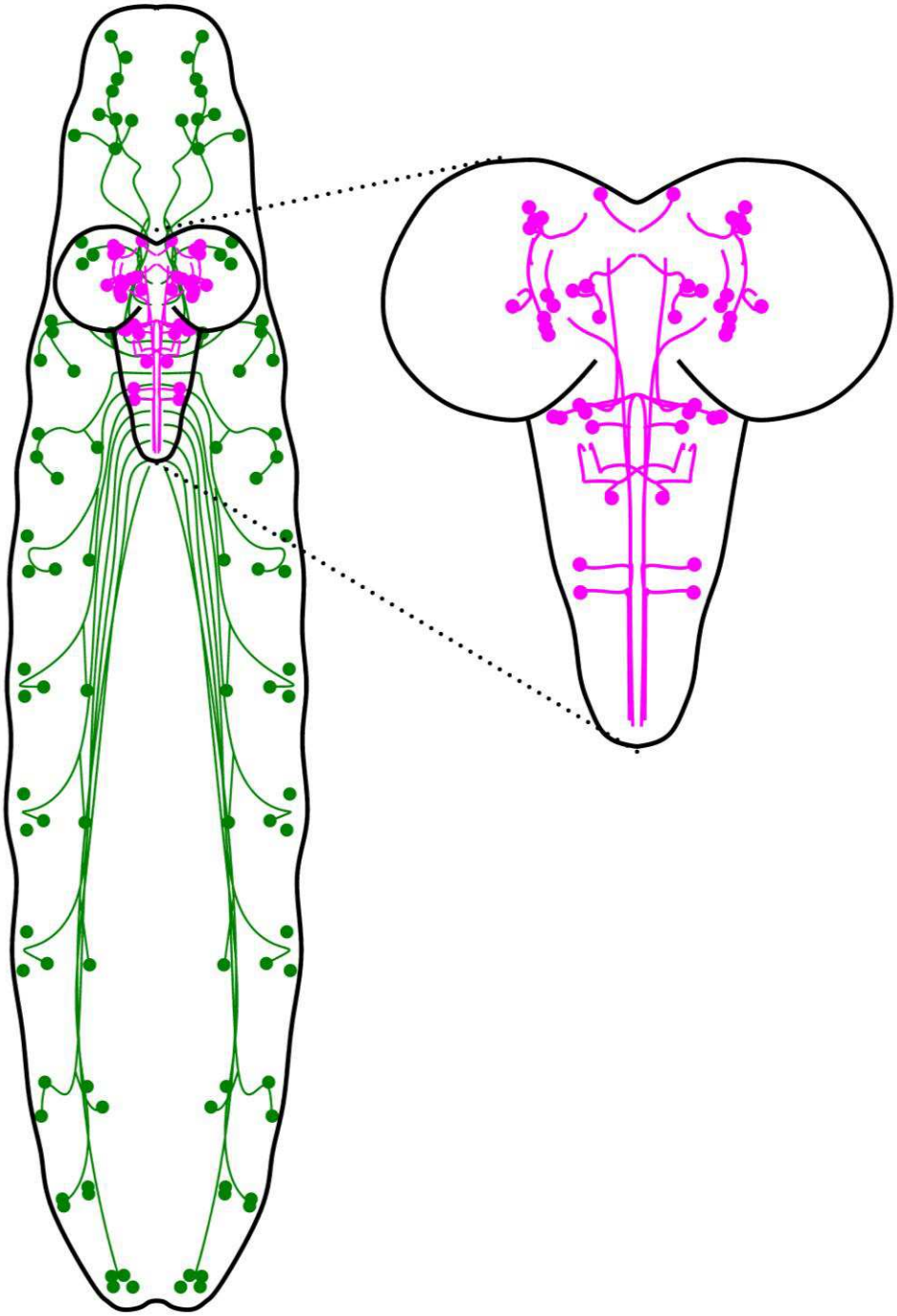

Figure 1. Schematic of *Drosophila* larva with heat sensing neurons. Green circles and lines indicate the type IV multidendritic neurons in the body wall. Pink circles and lines indicate the trpA1-AB neurons in the central nervous system. The zoom in view of the larval brain is shown on the right.

Reference

1. Scripture, E.W., *The new psychology*. 1905: Felling-o,-Tyne.
2. Heinzmann, *Ubeber die Wirkung sehr allmaliger Aenderungen thermischer Reize auf die Empfindungsnerven.* Archiv f. d. ges. Physiol (Pfluger), 1872. **vi. 222**.
3. Frasscher, *Ueber continuirliche und langsame Nervenreizung.* Jenaische Zeitschrift, 1875. **N. F. ii. I30**.
4. Sedgwick, *On the Variation of Reflex Excitability in the Frog induced by changes of Temperature.* Stud. Biol. Lab., Johns Hopkins Univ., 1882. **385**.
5. Morgan, A.H., *The Temperature Senses in the Frog's Skin.* The Journal of Experimental Zoology, 1922. **35**: p. 83.
6. Green, B.G. and C. Akirav, *Threshold and rate sensitivity of low-threshold thermal nociception.* Eur J Neurosci, 2010. **31**(9): p. 1637-45.
7. Story, G.M., *The emerging role of TRP channels in mechanisms of temperature and pain sensation.* Curr Neuropharmacol, 2006. **4**(3): p. 183-96.
8. Patapoutian, A., et al., *ThermoTRP channels and beyond: mechanisms of temperature sensation.* Nat Rev Neurosci, 2003. **4**(7): p. 529-39.
9. Caterina, M.J., et al., *The capsaicin receptor: a heat-activated ion channel in the pain pathway.* Nature, 1997. **389**(6653): p. 816-824.
10. Caterina, M.J., et al., *A capsaicin-receptor homologue with a high threshold for noxious heat.* Nature, 1999. **398**(6726): p. 436-441.

11. Viswanath, V., et al., *Opposite thermosensor in fruitfly and mouse.* Nature, 2003. **423**(6942): p. 822-823.

12. Zhong, L., R.Y. Hwang, and W.D. Tracey, *Pickpocket is a DEG/ENaC protein required for mechanical nociception in Drosophila larvae.* Curr Biol, 2010. **20**(5): p. 429-34.

13. Kang, K., et al., *Modulation of TRPA1 thermal sensitivity enables sensory discrimination in Drosophila.* Nature, 2012. **481**(7379): p. 76-80.

14. Tracey, W.D., Jr., et al., *painless, a Drosophila gene essential for nociception.* Cell, 2003. **113**(2): p. 261-73.

15. Lee, Y., et al., *Pyrexia is a new thermal transient receptor potential channel endowing tolerance to high temperatures in Drosophila melanogaster.* Nat Genet, 2005. **37**(3): p. 305-10.

16. Sokabe, T., et al., *Drosophila painless is a Ca2+-requiring channel activated by noxious heat.* The Journal of Neuroscience, 2008. **28**(40): p. 9929-9938.

17. McKemy, D.D., W.M. Neuhausser, and D. Julius, *Identification of a cold receptor reveals a general role for TRP channels in thermosensation.* Nature, 2002. **416**(6876): p. 52-8.

18. Story, G.M., et al., *ANKTM1, a TRP-like channel expressed in nociceptive neurons, Is activated by cold temperatures.* Cell, 2003. **112**(6): p. 819-829.

19. Kwon, Y., et al., *Fine thermotactic discrimination between the optimal and slightly cooler temperatures via a TRPV channel in chordotonal neurons.* J Neurosci, 2010. **30**(31): p. 10465-71.

20. Rosenzweig, M., K. Kang, and P.A. Garrity, *Distinct TRP channels are required for warm and cool avoidance in Drosophila melanogaster.* Proc Natl Acad Sci U S A, 2008. **105**(38): p. 14668-73.

21. Gallio, M., et al., *The coding of temperature in the Drosophila brain.* Cell, 2011. **144**(4): p. 614-24.

22. Shen, W.L., et al., *Function of rhodopsin in temperature discrimination in Drosophila.* Science, 2011. **331**(6022): p. 1333-6.

23. Kwon, Y., et al., *Control of thermotactic behavior via coupling of a TRP channel to a phospholipase C signaling cascade.* Nat. Neurosci., 2008. **11**: p. 871-873.

24. Sokabe, T., et al., *A Switch in Thermal Preference in Drosophila Larvae Depends on Multiple Rhodopsins.* Cell Rep, 2016. **17**(2): p. 336-344.

25. Ni, L., et al., *A gustatory receptor paralogue controls rapid warmth avoidance in Drosophila.* Nature, 2013. **500**(7464): p. 580-584.

26. Cho, H., et al., *The calcium-activated chloride channel anoctamin 1 acts as a heat sensor in nociceptive neurons.* Nature neuroscience, 2012. **15**(7): p. 1015-1021.

27. Xiao, B., et al., *Temperature-dependent STIM1 activation induces Ca2+ influx and modulates gene expression.* Nature chemical biology, 2011. **7**(6): p. 351-358.

28. Ni, L., et al., *The Ionotropic Receptors IR21a and IR25a mediate cool sensing in Drosophila.* Elife, 2016. **5**.

29. Akopian, A.N., et al., *Transient receptor potential TRPA1 channel desensitization in sensory neurons is agonist dependent and regulated by TRPV1-directed internalization.* J Physiol, 2007. **583**(Pt 1): p. 175-93.

30. Cordero-Morales, J.F., E.O. Gracheva, and D. Julius, *Cytoplasmic ankyrin repeats of transient receptor potential A1 (TRPA1) dictate sensitivity to thermal and chemical stimuli.* Proc. Natl. Acad. Sci. USA, 2011. **108**(46): p. E1184-91.

31. Gracheva, E.O., et al., *Molecular basis of infrared detection by snakes.* Nature, 2010. **464**(7291): p. 1006-11.

32. Basbaum, A.I., et al., *Cellular and molecular mechanisms of pain.* Cell, 2009. **139**(2): p. 267-284.

33. Jordt, S.-E., D.D. McKemy, and D. Julius, *Lessons from peppers and peppermint: the molecular logic of thermosensation.* Current opinion in neurobiology, 2003. **13**(4): p. 487-492.

34. Güler, A.D., et al., *Heat-evoked activation of the ion channel, TRPV4.* The Journal of neuroscience, 2002. **22**(15): p. 6408-6414.

35. Satinoff, E., *Neural organization and evolution of thermal regulation in mammals.* Science, 1978. **201**(4350): p. 16-22.

36. Hori, A., K. Minato, and S. Kobayashi, *Warming-activated channels of warm-sensitive neurons in rat hypothalamic slices.* Neuroscience letters, 1999. **275**(2): p. 93-96.

37. Hamada, F.N., et al., *An internal thermal sensor controlling temperature preference in Drosophila.* Nature, 2008. **454**(7201): p. 217-220.

38. Zhong, L., et al., *Thermosensory and nonthermosensory isoforms of Drosophila melanogaster TRPA1 reveal heat-sensor domains of a thermoTRP Channel.* Cell Rep, 2012. **1**(1): p. 43-55.

39. Hwang, R.Y., et al., *Nociceptive neurons protect Drosophila larvae from parasitoid wasps.* Curr Biol, 2007. **17**(24): p. 2105-16.

40. Chattopadhyay, A., A.V. Gilstrap, and M.J. Galko, *Local and global methods of assessing thermal nociception in Drosophila larvae.* J Vis Exp, 2012(63): p. e3837.

Chapter 2. TRPA1 mediates sensation of the rate of temperature change in Drosophila larvae

Results

Dependence of the nociceptive rolling response on the rate of temperature increase

In order to characterize the behavior of larvae in response to different rates of temperature change, we built an apparatus that allowed us to accurately control the heating speed, while monitoring larval movement. The temperature control system was comprised of a Peltier pad and a programmable integrated circuit responsible for voltage regulation. We used this apparatus to heat and cool an agarose surface for larval navigation. A video camera recorded the larvae behavior, and a computer program, MAGAT Analyzer [1], recognized the larvae in each frame.

To automatically and objectively analyze the large volume of data, we wrote an algorithm that employed several parameters to discern rolling from non-rolling larvae. These included the speed of the larvae, their direction of movement perpendicular to the body, acceleration, and acceleration perpendicular to the body. We used a machine learning [2, 3] approach to successively improve the ability of the computer to accurately identify rolling larvae, with minimal noise.

We exposed wild-type 2nd instar larvae to temperature ramps with different slopes, and determined the dependence of rolling on the rate of temperature change (dT/dt). In each experiment, we initially maintained the temperature at ~23.5 °C for 30 seconds and then increased the temperature to 40 °C. Larvae rolled when the temperature increased quickly (0.3 °C/s). As the temperature approached 40 °C, the larvae stopped moving and the rolling behavior ceased (**Fig. 1a**). However, the animals still responded to a mechanical stimulus.

We calculated the fraction of larvae displaying rolling behavior using two parameters: F_{peak} and T_{middle}. F_{peak} was the maximum fraction of larvae that rolled during the temperature ramp. T_{middle} was the temperature in which the fraction of rolling was halfway between the baseline rolling behavior (at the start of the experiment) and F_{peak}. We found that the relation between rolling and temperature (T) was dependent on the rate of temperature change. When the temperature rose at the fastest rate tested (0.5 °C/s), the maximum fraction of larvae that rolled (F_{peak}) was 0.89 ±0.09, and the T_{middle} temperature was 29.1 ±0.3 °C (**Fig. 1a,j,k**). As the rate of temperature change declined, the F_{peak} decreased, and the T_{middle} rose (**Fig. 1b-k**). At the slowest rate examined (0.02 °C/s), the F_{peak} fell to 0.47 ±0.08, and the T_{middle} increased to 34.5 ±0.6 °C (**Fig. 1j,k**). Thus, when the rate of temperature increase was very gradual, only about half as many larvae rolled at a temperature that was >5 °C hotter. These results demonstrate that under conditions in which the temperature rose slowly, the tendency for the larvae to initiate an escape response was diminished greatly.

Requirement for TRPA1-A for heat-induced rolling

To identity a channel that might enable larvae to sense the fast temperature increases that stimulate rolling behavior, we screened for mutations in genes encoding channels known to detect temperatures in the noxious heat range (*trpA1*, *painless* and *pyx*) [4-10]. We found that $trpA1^{1}$ mutant flies exhibited severe defects in heat-induced rolling behavior (**Fig. 2a,b**, **Supplementary Fig. 1**), and this phenotype was suppressed by a duplication that included the wild-type *trpA1* gene

(**Fig. 2c**). In contrast, the *pain*^{2} and *pyx*^{3} mutations had no or minimal effects in this temperature change assay (**Fig. 2d,e**), although loss of *painless* has been reported to elevate the threshold for a thermal escape response from 29 ° to 33 °C [11]. We also found that *Gr28b*^{MB03888}, a mutation affecting a receptor protein required for sensing innocuously warm temperatures [12], did not significantly impact on rolling behavior (**Fig. 2f**).

The *trpA1* gene encodes four mRNA isoforms: *trpA1-A*, *B*, *C* and *D* (**Fig. 3a**) [9, 13]. The *trpA1-A* and *trpA1-B* isoforms (*trpA1-AB*) share one promoter and the *trpA1-C and trpA1-D* isoforms (*trpA1-CD*) share another promoter[9]. *trpA1-A* and *trpA1-D* have a common exon (**Fig. 3a**; boxes with diagonal lines), which enables them to be activated by elevated temperatures. The different N-termini in TRPA1-A and TRPA1-D influence their temperature thresholds (25 °C for TRPA1-A and 36 °C for TRPA1-D) [9, 14].

To determine which TRPA1 isoform was required for heat-induced rolling, we first assessed the effects of knocking out each isoform pair (*trpA1-AB* and *trpA1-CD*). To address the requirements for the TRPA1-AB, we took advantage of the *trpA1-AB*^{GAL4} allele, which eliminates TRPA1-A and TRPA1-B [15]. To disrupt TRPA1-CD, we used homologous recombination to create an allele containing a *GAL4* reporter in place of 732 nucleotides spanning the *trpA1-CD* translation initiation codon (**Fig. 3a**). We then exposed the mutant larvae to a temperature heat ramp (0.1 °C/s). We found that the *trpA1-AB*^{GAL4} larvae displayed significantly reduced rolling behavior, indicating that either the A or B isoform was required

(**Fig. 3b**). In contrast, the *trpA1-CD*^{GAL4} larvae showed rolling behavior that was more reminiscent of the control larvae (**Fig. 3c**).

To address whether TRPA1-A or TRPA1-B was required for heat-induced nociception, we deleted two nucleotides in the exon that were present in *trpA1-A*, but not in *trpA1-B* (**Fig. 3a**; exons labeled with diagonal lines). We introduced this mutation (*AD**) in the *trpA1-CD*^{GAL4} background using the CRISPR/Cas9 system [16-19]. In this mutant, only the *B* isoform of *trpA1* remained (*trpA1-ACD*^{GAL4}). We found that *trpA1-ACD*^{GAL4} displayed a deficit in responding to the heat ramp, similar to *trpA1-AB*^{GAL4} flies (**Fig. 3b,d**). These findings indicated in this assay the key temperature sensor required for inducing rolling behavior was *trpA1-A*.

We attempted to rescue the *trpA1-AB*^{GAL4} mutant phenotype by expressing *trpA1-A* in *trpA1-AB* neurons. However, driving *trpA1-A* expression in *trpA1-AB* neurons decreased the T_{middle} to 27.0 ±0.2 °C (0.1 °C/s), which was ~5 °C lower than control animals (31.9 ±0.5 °C; **Supplementary Fig. 2a,b**). This increased rolling behavior at lower temperatures suggested that the threshold for this avoidance behavior might be sensitive to expression levels, since the *GAL4/UAS* system potentially drove higher expression levels than the endogenous *trpA1* promoter. Moreover, the rolling declined and then ceased at a lower temperature than control flies due to an increasing proportion of heat-induced locomotor arrest. (F_{peak}: control, 0.90 ±0.06; *UAS-trpA1-A/+*; *trpA1-AB*^{GAL4}*/trpA1*^{1}, 0.35 ±0.05). We observed a similar effect of expressing *trpA1-A* in a heterozygous background (*UAS-trpA1-A/+*;*trpA1-AB*^{GAL4}*/+*; **Supplementary Fig. 2d;** F_{peak} = 0.44 ±0.03; T_{middle} = 25.9 ±0.2 °C). In contrast to the effects of driving expression of *trpA1-A*,

we found that introducing *trpA1-B* in *trpA1-AB* neurons had no effect (**Supplementary Fig. 2c**).

To determine whether ectopic expression of *trpA1-A* could endow sensitivity to the rate of temperature change, we expressed *trpA1-A* in class IV multidendritic neurons (mdIV neurons) in a $trpA1^{1}$ mutant background (*UAS-trpA1-A/ppk-GAL4*;$trpA1^{1}$; **Supplementary Fig. 3**). The $trpA1^{1}$ null mutant larvae or $trpA1^{1}$ larvae harboring only the *ppk-GAL4* or the *UAS-trpA1-A* transgene were virtually unresponsive to slow or fast temperature ramps (**Supplementary Fig. 3a,j**). However, upon applying a fast heat ramp (0.5 °C/s) to larvae ectopically expressing *UAS-trpA1-A* under control of the *ppk-GAL4*, the fraction of animals that rolled (F_{peak}) was 0.75 ±0.01 (**Supplementary Fig. 3a,j**). As the rate of temperature change declined, the F_{peak} decreased (**Supplementary Fig. 3b-j**). At the slowest rate examined (0.02 °C/s), the F_{peak} fell to 0.35 ±0.04 (**Supplementary Fig. 3i,j**). However, the T_{middle} was not significantly different (**Supplementary Fig. 3k**).

trpA1-AB neurons critical for sensing rapid temperature change

We performed homologous recombination using the CRISPR/Cas9 system [16-19] to introduce the *LexA* gene into the *trpA1-AB* translation initiation codon, so that we could subsequently use this $trpA1\text{-}AB^{LexA}$ reporter in combination with *GAL4* reporters (**Fig. 3a**). The *LexA* gene and the w^{+} marker replaced the same genomic region as in $trpA1\text{-}AB^{GAL4}$ [15]. The *trpA1-AB LexA* reporter ($trpA1\text{-}AB^{LexA}$/+) was expressed in a variety of neurons in the brain and ventral nerve cord (VNC) (**Fig. 4a,b** and **Supplementary Fig. 4**). We observed an indistinguishable

expression pattern in the *trpA1-AB*^{LexA} homozygous larvae (**Supplementary Fig. 4a,b** and **Supplementary Fig. 5**) indicating that the *trpA1-AB* phenotype was not due to loss of the *trpA1-AB*-expressing neurons.

To determine the specific *trpA1-AB* expressing neurons required for rolling, we used RNAi-mediated gene silencing to assess the effects of knocking down *trpA1* expression in different subsets of *trpA1-AB* neurons. To identify *GAL4* lines to conduct the RNAi screen, we took advantage of the *trpA1-AB*^{LexA} reporter to test for overlap, by performing co-labeling and intersectional FLP-out strategies. The *GAL4* lines we screened were from the Bloomington Drosophila Stock Center (BDSC) that label neurotransmitter- or neuropeptide-releasing neurons. We also reviewed the staining patterns of the Janelia collection of ~7000 *GAL4* lines by employing an image processing program we wrote to narrow down the candidates, and then manually checked their expression patterns. Furthermore, we combined *GAL80* lines from the BDSC with the *trpA1-AB*^{GAL4} reporter to label a subset of *trpA1-AB* neurons.

We identified ~70 candidate *GAL4* lines, which might overlap with the *trpA1-AB*^{GAL4}. To clearly detect the neurons that expressed the *GAL4* and the *trpA1-AB*^{LexA} reporters, we used a "flipped out" approach. We crossed the *GAL4* lines into a genetic background such that the *trpA1-AB*^{LexA} positive neurons that did not express a given *GAL4* were marked by mCherry. If the *trpA1-AB*^{LexA} positive neurons also expressed *GAL4*, then the mCherry cassette was removed genetically flipped out, thereby leading to expression of the Citrine marker. We found six *GAL4* lines that overlapped with fewer than 10 pairs of *trpA1-AB*^{LexA} positive neurons (**Fig. 4c**,

Supplementary Fig. 6 and **Supplementary Fig. 7**), and were therefore useful tools to manipulate small subsets of *trpA1-AB*^{LexA} positive neurons.

We examined the requirements for different *trpA1-AB* neurons for rolling behavior in response to noxious heat by knocking down *trpA1* expression by RNAi. We then performed temperature ramps at 0.1 °C/s and measured the F_{Peak}. Knockdown of *trpA1* using the *R60F07-GAL4* elicited severe rolling deficits (**Fig. 4d** and **Supplementary Fig. 8a**). The *R60F07-GAL4* was expressed in just three of the twelve classes of *trpA1*-positive neurons: brain lateral central (BLC) neurons, brain lateral posterior (BLP) neurons and VNC anterior posterior (VAP) neurons (**Fig. 4b,c** and **Supplementary Fig. 7a-c**). The *386Y-GAL4*, which overlapped with *R60F07* in only the BLP class (**Fig. 4b,c** and **Supplementary Fig. 7d-f**), also caused strong impairment in rolling, when we used it to knockdown *trpA1* (**Fig. 4d** and **Supplementary Fig. 8b**). The *tsh-GAL80*;*trpA1-AB*^{GAL4} only labeled *trpA1-AB* BLP neurons (**Fig. 4b,c** and **Supplementary Fig. 6g-i**). Using this latter *GAL4* in combination with the *tsh-GAL80* to knock-down *trpA1* expression reduced the F_{peak} significantly compared to control and *trpA1-AB*^{GAL4}/+ (**Fig. 4d** and **Supplementary Fig. 8c,d**). We did not observe a significant reduction in rolling behavior after suppressing *trpA1* using any of three *GAL4* lines that were not expressed in BLP neurons (**Fig. 4b-d**; **Supplementary Fig. 7** and **Supplementary Fig. 8e-g**). Thus, we conclude that expression of *trpA1* in BLP neurons influences rolling behavior.

To test whether BLP were sufficient to trigger rolling behaviors, we performed optogenetic experiments. We found that expression of *UAS-CsChrimson* [20] under

control of the *trpA1-AB*^{GAL4} (*UAS-CsChrimson/CyO*;*trpA1-AB*^{GAL4}) triggered rolling behavior but not paralysis (**Fig. 4e**). Using the *tsh-GAL80*, we suppressed *trpA1-AB*^{GAL4}-dependent expression of *UAS-CsChrimson,* but retained expression in two of the three BLP neurons (**Supplementary Fig. 6g-i**). We found that light also triggered rolling in these larvae (**Fig. 4e**), but not in control larvae harboring *UAS-CsChrimson/+* alone (**Fig. 4e**).

trpA1-AB and *trpA1-CD* neurons function in a common circuit

We showed above that *trpA1-AB* was required for the rolling behavior evoked by rapid heating of the entire larvae body. However, the *trpA1-CD* neurons expressing *trpA1-C* and *painless* are necessary for the rolling induced by touching a localized spot on the larvae with a hot (>39 °C) probe [5, 9]. Even though the temperature thresholds were different, *trpA1-AB* neurons and *trpA1-CD* neurons both trigger rolling behavior in response to noxious heat. This raises the possibility that the *trpA1-AB* and *trpA1-CD* neurons function in a common neuronal circuit.

In order to determine the relative expression patterns of the *trpA1-AB* and *trpA1-CD* neurons, we performed double-labeling experiments. The *trpA1-CD*^{GAL4}/+ reporter stained mdIV neurons in the body wall (**Fig. 5a**), which extended axonal projections to the ventral nerve cord (VNC) (**Fig. 5b**). In contrast, the *trpA1-AB*^{LexA}/+ reporter stained neurons in the larval brain and VNC, but not in body wall neurons (**Fig. 4a and Fig. 5b**). Therefore, there was no apparent overlap between the expression patterns for the *trpA1-AB* and *trpA1-CD* reporters.

Since the localization of *trpA1-AB* neurons and *trpA1-CD* neurons were close to each other in the VNC, we wondered whether they formed synapses. GFP reconstitution across synaptic partners (GRASP) is a system to label membrane contacts between two cells in living animals [21]. We used *trpA1-AB*^{LexA} and *trpA1-CD*^{GAL4} to drive *LexAop-CD4::spGFP11* and *UAS-CD::spGFP1-10* and found that they form functional GFP in the VNC (**Fig. 5c**). These results indicate that *trpA1-CD* and *trpA1-AB* neurons are in close proximity, and possibly form synaptic connections.

BLP *trpA1-AB* neuronal activity increased by steep temperature ramps

The *trpA1-AB* neurons in the central nervous system (CNS) might directly sense the rate of temperature change. Alternatively, these brain neurons may not be thermally activated, but receive signals from temperature-activated peripheral neurons. Drosophila TRPA1 is a Ca^{2+}-permeable channel[4]. To monitor Ca^{2+} increases in response to different rates of temperature change, we expressed *UAS-GCaMP6f* [22] under the control of the *trpA1-AB*^{GAL4} (*trpA1-AB*^{GAL4}/+), and dissected out the CNS from the transgenic larvae. We varied the temperature ramps from 0.05 to 0.2 °C/s and monitored the changes in fluorescence ($\Delta F/F_o$). We found that the rise of Ca^{2+} in BLP neurons correlated with the steepness of the temperature ramps (0.2 °C/s, $\Delta F/F_o$ = 4.9 ±1.0; 0.1 °C/s, $\Delta F/F_o$ = 3.2 ±0.6; 0.05 °C/s, $\Delta F/F_o$ = 1.7 ±0.2; **Fig. 6a,b,d,e,g,h**. $p = 4.7 \times 10^{-7}$ by one-way ANOVA). The Ca^{2+} increase was due to TRPA1, since it was eliminated in *trpA1-AB*^{GAL4} homozygous mutant flies (**Fig. 6j,k**). The BLA neurons also showed Ca^{2+} changes in response to the

faster ramps (**Fig. 6c,f,i,l**), and were eliminated in the *trpA1-AB*^{GAL4} mutant (**Fig. 6l**). However, the peak responses of the BLA neurons were much smaller than those exhibited by the BLP neurons (**Fig. 6c,f,i**). These findings indicate that TRPA1-AB expressing neurons are activated by rapid temperature changes, and that the BLP neurons respond most robustly, especially when the rate of temperature change was the most rapid. Consistent with the conclusion that BLP and BLA are intrinsically responsive to temperature, these neurons also responded to temperature in the presence of tetrodotoxin (TTX; **Supplementary Fig. 9**), which depresses synaptic transmission due to blocking voltage-gated Na^+ channels and nerve conduction.

TRPA1-A activity enhanced by rapid changes in temperature

To address whether TRPA1 was sensitive to the rate of temperature change, we expressed TRPA1-A in *Xenopus* oocytes and performed two-electrode voltage clamp experiments. We increased the temperature at either slow (0.05 ±0.02 °C/s) or fast (0.2 ±0.02 °C/s) rates and measured the currents (24 °C to 35 °C for TRPA1-A, 24 °C to 40 °C for TRPA1-D). When the temperature increased slowly, the peak current was -1.2 μA (**Fig. 7a,b**). However, when we employed the steeper temperature ramp, the peak current increased ~3-fold to -3.7 μA (**Fig. 7a,b**). Q_{10} is defined as the fold increase in activity caused by a 10 °C rise in temperature. In each pair of experiments, the Q_{10} increased significantly with the faster temperature changing rate (p = 6.1 x 10^{-5}; **Fig. 7c**). This suggested that the activity of the TRPA1-A channel was controlled both by the rate of temperature increase, and by the absolute temperature. While the peak current was much larger during the fast

heat ramp, there was more total current (charge) during the slow ramp (**Supplementary Fig. 10**). Nevertheless, we suggest that the peak current is the more relevant parameter since the lower peak during the slow ramp may be insufficient to cross the threshold to trigger action potentials.

We tested whether Ca^{2+} affected the differences in Q_{10} during the slow and fast temperature ramps, as well as the absolute Q_{10}s under both conditions. When we eliminated Ca^{2+} from the external bath, the differences in Q_{10} at the slow and fast rates were not significant ($p = 0.16$; **Fig. 7d**). However, the Q_{10} values were much higher than in the presence of Ca^{2+} (**Fig. 7c,d**). These findings suggest that inactivation of TRPA1-A is sensitive to Ca^{2+}, as is the case for mammalian TRPA1 [23-26].

In addition to TRPA1-A, one additional TRPA1 isoform, TRPA1-D, is thermosensitive [9, 14]. We found that TRPA1-D also exhibited a higher Q_{10} in response to the faster temperature ramp ($p = 0.034$; **Fig. 7e**). However, the differences between the slow and fast ramps were not as significant as with TRPA1-A (**Fig. 7c**). Thus, the N-terminal exons that are distinct between dTRPA1-A and -D (**Fig. 3a**) may contribute to the magnitude of the sensitivity to rate of temperature change. We also tested whether rat TRPV1 (rTRPV1) is sensitive to the rate of temperature change. Reminiscent of TRPA1, rTRPV1 also exhibited significant differences in Q_{10} using slow and fast temperature ramps ($p = 0.014$, **Fig. 7f;** 24 °—48 °C ramp).

Discussion

We established Drosophila larvae as an animal model for dissecting the physiological basis through which an animal displays nociceptive behavior in proportion to the rate of heating. We found that if the temperature rose quickly, a much greater percentage of larvae initiated an escape response, which involved rolling perpendicular to its body axis. Moreover, they did so at much higher temperatures if the environmental temperature increased slowly. Thus, we conclude that Drosophila larvae also respond to the rate of heating, rather than just the absolute temperature.

We demonstrated that the molecular sensor essential for detecting the rate of temperature change was a TRPA1 isoform, TRPA1-A. The peak TRPA1-A-dependent currents were larger when the heating was rapid, demonstrating that the activity of this thermoTRP was not strictly a function of the actual temperature, but was also impacted by the heating rate. This finding was consistent with the larval behavioral response to different heating slopes. Rapid heating not only increased the percentage of larvae that roll, but decreased the temperature at which the nociceptive behavior took place.

The *trpA1-A*-expressing neurons that were critical for sensing the heating speeds were in the brain. In support of this conclusion, the *trpA1-AB* reporter (*trpA1-AB*^{GAL4}) expressed in the brain in BLP neurons. Using a genetically encoded Ca^{2+} sensor, we found that BLP neurons exhibited larger Ca^{2+} responses when they were heated rapidly. The heat-induced Ca^{2+} signals were eliminated in *trpA1-AB* mutant larvae. Nevertheless, we cannot exclude that voltage-gated Ca^{2+}-channels

activated subsequent to TRPA1 contribute to the rise in Ca^{2+}. Because the tissue that we used for these experiments were devoid of the peripheral nervous system, our data indicate that that the BLP neurons are directly sensing the rate of temperature change. Moreover, these neurons responded to temperature changes in the presence of TTX, which suppresses voltage-gated Na^{+} channels and synaptic transmission.

Neural accommodation is a potential mechanism through which BLP neurons could respond differentially to variations in rate of temperature change. Neural accommodation is a consequence of inactivation of voltage-gated Na^{+} channels, due to slow depolarization. However, the slow depolarization that leads to neural accommodation typically occurs on a sub-second timescale [27], and our fastest temperature ramps (0.5 °C/s) occurred over the course of many seconds. Thus, we suggest that the lower rolling propensity in response to the slow temperature ramps are not likely due neural accommodation, although our data do not formally rule this out. Nevertheless, a more likely mechanism is Ca^{2+}-dependent inactivation of the TRPA1 channels themselves. Consistent with this latter possibility, we found that the peak TRPA1-A currents were similar in response to slow and fast heat ramps in the absence of external Ca^{2+}. However, during slow heat ramps in the presence of external Ca^{2+}, there is more time for Ca^{2+} to inactivate the TRPA1 channels, thereby reducing the peak currents.

In addition to a role for *trpA1-AB*-expressing BLP neurons in thermal nociception, *trpA1-CD*-positive neurons in the periphery also sense elevated temperatures [9]. However, the activation threshold for *trpA1-AB* neurons in the

central brain is considerably below the temperature required for activation of the *trpA1-CD* neurons in the periphery, which is >40 °C[9]. Nevertheless activation of either group of neurons elicits the same rolling behavior. Based on the GRASP analysis, it appears that the *trpA1-AB* and *trpA1-CD* neurons are in close proximity, suggesting that these neurons might function in a common neuronal circuit. Thus *trpA1-AB* neurons in the larval brain are not only primary thermosensors, but may also be transducers of peripheral signals.

We propose that having two groups of thermosensory neurons offers a dual defense. One class, the central brain *trpA1-AB* neurons, has a low threshold when heating is precipitous, thereby enabling the larvae to begin detecting rapid rates of temperature increase before the temperature rises to an acutely dangerous level. The faster the rate of temperature increase the lower the threshold, thereby providing the animals amble time to initiate rolling and escape a noxious environment. However, if the rate of temperature increase is very gradual, the larvae have more time to respond and do not need to initiate an abrupt escape. Once the absolute temperature reaches an acutely noxious temperature, such as 39 °C, activation of the *trpA1-CD* neurons stimulates a rolling response, thereby providing a second line of defense, via activation of the same neuronal circuit. Nevertheless, another TRP channel, referred to as Painless participates in thermal nociceptive responses [5, 11]. Thus, this TRP might provide a distinct backup mechanism that allows the animals to respond to noxious temperature changes. Finally, our findings that the robust behavioral response of larvae to rapid heating is mediated by a low-

threshold TRP channel raise questions as to whether similar mechanisms occur in vertebrate animals, ranging from amphibians to mammals.

Experimental Procedures

Fly stocks

We used the following flies that were described previously: *UAS-CD4::spGFP1-10, LexAop-CD4::spGFP11* [21], *trpA1-AB^{GAL4}* [15], *UAS-trpA1-A* [28], *UAS-trpA1-B* [29], *pain^{2}* [5], *pyx^{3}* [6], *Gr28b^{MB03888}* [30],*trpA1-BAC* [9], *ppk-GAL4* [31], *UAS-kir2.1* [20, 32], *tsh-GAL80* [33]. We obtained the following flies from the Bloomington Drosophila Stock Center: *UAS-mCD8::GFP* (BDSC #52261) [34], *UAS-FLP* (BDSC #4539) [35], *LexAop-frt-mCherry-STOP-frt-ReaChR::Citrine* (BDSC #53745) [36], *UAS-GCaMP6f* (BDSC #42747) [22], *386Y-GAL4* (BDSC #25410) [37], *R60F07-GAL4* (BDSC #45358) [38], *R21E09-GAL4* (BDSC #48948) [39], *R21G01-GAL4* (BDSC #48951) [38] and *R21F01-GAL4* (BDSC #49862) [38], *UAS-CsChrimson* (BDSC #55135) [20].

Assaying temperature induced rolling behavior in 2nd instar larvae

The camera and illumination system that we built was similar to that described previously [40]. Briefly, it consisted of a 12 cm x 12 cm temperature control apparatus, which we assembled with nine 4 x 4 cm sections of a VT-127-1.4-1.15-71 Peltier device (TE Technology). The power controller for the Peltier device was a TC-36-25-RS232 temperature controller (TE Technology) (**Supplementary Fig. 11**). We also wrote a LabView program to drive the temperature controller and synchronized it to the recording camera. The scripts will be provided upon request.

To obtain 2nd instar larvae, we collected embryos for 4-6 hours and incubated them for 72 hours at 25 °C under 12 h light/12 h dark cycles. We tested their

behaviors during the light cycle. We also tested wild type 3rd instar larvae (96h hours at 25 °C) and found that their rolling behaviors in response to heat ramps were similar to 2nd instar larvae (**Supplementary Fig. 12**). We focused our analyses on 2nd instar larvae in most of our behavioral experiments. Due to the small body size of 2nd instar larvae (<1 mm in diameter), the temperature of their brain was almost the same as the environment. The temperature differential between the center of the larva and the surrounding environment was <0.05 °C when temperature was increased at a rate of 0.1 °C/s [41].

Before initiating the experiments, we separated the larvae from the food by washing in 15% sucrose. The density of the 15% sucrose solution is higher than the larvae but lower than the density of fly food. Thus, the larvae float above the sucrose, while the fly food sinks to the bottom. We skimmed the larvae from the top of the sucrose solution and washed them with water to remove the residual sucrose. Using a paint brush, we distributed ≥30 larvae evenly on the 12 cm x 12 cm Peltier pad coated with 1 mm thick 2% agarose in water. The larvae were not selected by their gender in the behavior experiments. We kept the surface of the agarose moist by spreading enough water on the Peltier pad to lubricate the larvae during the experiments. For each experimental condition, we repeated the behavior experiments on ≥3 groups of larvae.

We used MAGAT Analyzer [1] to recognize the larvae in each frame and calculated several parameters to discern rolling from non-rolling larvae. These included the speed of the larvae, the speed perpendicular to the body, acceleration, and acceleration perpendicular to the body. We then created a machine-learning

algorithm, which after several iterations of manual feedback, accurately discerned rolling from non-rolling larvae automatically.

We employed four steps to construct a computer program to recognize larval rolling behaviors [2, 3]. 1) We manually recognized rolling behaviors using batches of larval tracking data from different temperature ramp experiments. The experimental data included control flies (w^{1118}) and *trpA1-AB*^{GAL4} mutant 2nd instar larvae exposed to rapid (0.2 °C/s) or slow (0.02 °C/s) temperature ramps. 2) During the learning step, we input the above raw data into our computer program and optimized a variety of parameters, such as velocity, acceleration and speed perpendicular to the body, so that the discrimination between rolling and non-rolling larvae was most similar to our manual recognition. 3) To test the effectiveness of the program, we input another test batch of larval tracking data into our optimized program and checked whether the program distinguished rolling from non-rolling larvae. 4) During the quality-check step, we checked whether the discrimination results that we obtained from the computer program were similar to our manual discrimination of rolling versus non-rolling by evaluating 7479 data points. On the basis of this comparison, we found that the machine learning algorithm led to <1% false positives (0.87%) and ~5% false negatives (5.25%).

We defined the fraction of rolling larvae ($F_{rolling}$) using the following relation: $N_{rolling}/N_{total}$. $N_{rolling}$ was the number of rolling larvae and N_{total} was the total number of larvae. We defined F_{peak} as the maximum rolling fraction and T_{middle} as the temperature at which the rolling fraction was half the F_{peak}.

Generation of *trpA1* alleles

The *trpA1-CD^{GAL4}* allele, which we generated by homologous recombination [42], contained a 732 nucleotide deletion that spanned the translation initiation codon common to the *trpA1-C* and *trpA1-D* isoforms (**Fig. 2j**). To create the *trpA1-CD^{GAL4}*, we subcloned two 3-kb *trpA1* genomic DNA fragments into pw35*GAL4* [43] and used this plasmid to generate transgenic flies (BestGene). We crossed the transgenic flies with *hs-FLP* transgenic flies to generate the targeted allele as described [42]. We confirmed the *trpA1-CD^{GAL4}* allele by PCR (**Supplementary Fig. 13a, b**).

The *trpA1-AB^{LexA}* allele contained a 178 nucleotide deletion spanning the *trpA1-AB* translation initiation codon, which was identical to the deletion in *trpA1- AB^{GAL4}* [15]. The *trpA1-ACD^{GAL4}* allele contained the same deletion in *trpA1-CD^{GAL4}*, plus a two nucleotide deletion in the exon common between *trpA1-A* and *trpA1-D* (**Fig. 3a**). Consequently, *trpA1-ACD^{GAL4}* did not express the *trpA1-A*, *trpA1-C* or the *trpA1-D* isoforms. We generated both *trpA-AB^{LexA}* and *trpA1-ACD^{GAL4}* using the CRISPR/Cas9-system [16-19]. To generate the *trpA-AB^{LexA}* allele, we subcloned two 1-kb *trpA1* genomic DNA fragments into pBP*LexA::p65* [38], co-injected this plasmid along with pU6-*trpA1-AB*-chiRNA (targeting the first exon of *trpA1-AB*) into embryos of *Cas9* transgenic flies (BestGene). To confirm the *trpA1-AB^{LexA}* allele, we performed PCR to verify the insertion of the w^+ marker in the *trpA1* gene (**Supplementary Fig. 13a,c**). To generate the *trpA-ACD^{GAL4}* allele, We constructed the pU6-*trpA1-AD*-chiRNA plasmid by inserting a 20 bp guide sequence targeting to the 13th exon of *trpA1* into pU6-BbsI-chiRNA [18]. After injecting pHsp70-Cas9

and pU6-*trpA1-AD*-chiRNA into the *trpA1-CD*^{GAL4} allele (BestGene), we screened for the targeted mutant by qPCR and further confirmed the successful targeting by sequencing the corresponding genomic region (**Supplementary Fig. 13a,d**).

Immunohistochemistry

We used two strategies, "co-labeling" and "flip out", to identify *GAL4* lines that were co-expressed with the *trpA1 LexA* reporter (*trpA1-AB*^{LexA}). To perform the co-labeling strategy, we crossed each *GAL4* line to *UAS-mCD8::GFP*;*trpA1-AB*^{LexA},*LexAop-frt-mCherry-frt-ReaChR::Citrine* and surveyed for co-expression of the GFP and mCherry reporters. A limitation of this strategy was that it was challenging to assess whether the *GAL4* reporter overlapped with the *LexA* reporter, when the *GAL4* line labeled many neurons. In these cases, we performed the flip out strategy by crossing the *GAL4* lines with *UAS-FLP*;*trpA1-AB*^{LexA},*LexAop-frt-mCherry-frt-ReaChR::Citrine*. The *trpA1-AB*^{LexA} positive neurons that did not express the given *GAL4,* were marked by mCherry. If the *trpA1-AB*^{LexA} positive neurons also expressed *GAL4*, then the mCherry cassette flipped out, thereby leading to expression of the Citrine marker. However, a limitation of the flip out strategy is that the mCherry cassette flipped out stochastically. Therefore, we employed this latter strategy only when the co-labeling strategy was ineffective.

To perform the immunostaining, we dissected 3rd instar larvae and fixed them with 4% paraformaldehyde in PBST (154 mM NaCl, 5.60 mM Na_2HPO_4, 1.05 mM KH_2PO_4, and 0.3% Triton X-100; pH 7.4) at room temperature for 15 minutes. We washed the fixed larvae in PBST and blocked them with 5% normal goat serum

(NGS) in PBST. To perform the co-labeling experiments, we incubated the larvae overnight at 4 °C with chicken anti-GFP (1:500; Cat. #A10262, Invitrogen), which recognized either GFP or Citrine, and rabbit anti-DsRed (1:500; Cat. #632496, Clontech), which detected mCherry. After washing 3x in PBST, we incubated the samples overnight at 4 °C with the following secondary antibodies: 1) Alexa Fluor 488 goat-anti-chicken IgG (1:1000; Cat. #A11039, Invitrogen), and 2) Alexa Fluor 555 donkey-anti-rabbit IgG (1:1000; Cat. #A31572, Invitrogen). We imaged the samples using a Zeiss LSM700 Confocal Laser Scanning Microscopy using a 20x/0.8 Plan-Apochromat DIC objective, and Zen software. For each immunohistochemistry image shown, we gathered ≥3 images from different animals.

Optogenetic stimulation of larvae

To activate the *trpA1-AB* neurons or *trpA1-AB* BLP neurons by light, we expressed *UAS-CsChrimson* [20] under control of the *trpA1-AB*^{GAL4} [15] or the *tsh-GAL80*;*trpA1-AB*^{GAL4}. We used two copies of *trpA1-AB*^{GAL4} to increase the expression level of *UAS-CsChrimson* (*UAS-CsChrimson/*CyO;*trpA1-AB*^{GAL4}). We generated *UAS-CsChrimson/tsh-GAL80*;*trpA1-AB*^{GAL4} flies by crossing *UAS-CsChrimson/*CyO;*trpA1-AB*^{GAL4} males with *UAS-tsh-GAL80*;*trpA1-AB*^{GAL4} virgins. This cross produced two genotypes of larvae: *UAS-CsChrimson/tsh-GAL80*;*trpA1-AB*^{GAL4} and *tsh-GAL80/CyO*;*trpA1-AB*^{GAL4}. We kept the individual larvae tested in the optogenetics experiments until the adult stage to determine their genotypes.

We fed 1st instar larvae food containing all-*trans*-retinal, which we prepared by adding 50 μl of 100 mM all-*trans*-retinal to 5 ml of fly food, and then allowed the animals to grow until the 2nd instar larval stage. To conduct the experiments, we placed the larvae on a 2% agarose plate and stimulated the animals for 60 sec with red light from an AmScope HL250YA 150W Fiber Optic Dual-Gooseneck Stereo Microscope Light Illuminator. In order to obtain the red light, we used an AmScope CF-4 Color Filter for the Fiber Microscope Illuminator. The light intensity was 5.2 mW/cm^2. We recorded single larval behavior using an AmScope 7X-45X trinocular stereo zoom microscope and a Basler acA2000-165uc camera, and manually score its rolling behavior under light stimuli (roll: score = 1; not roll: score = 0).

Blinding and randomization

To score rolling behavior in a blind fashion, we devised a computer algorithm to score the behavior without human intervention. To analyze control, mutant and transgenic flies, we selected animals in a random fashion. To perform the optogenetic experiments (Fig. 4e), we randomly permuted all of the videos and recognized the rolling behaviors manually without knowledge of the genotypes.

GCaMP imaging to assay changes in Ca^{2+} in response to different d*T*/d*t*

To assay the activities of BLP and BLA neurons in response to different d*T*/d*t*, we expressed *UAS-GCaMP6f* [22] under control of the *trpA1-AB^{GAL4}* [15]. We focused this analysis on 3rd rather than 2nd instar larvae since both they both exhibit similar thermal nociceptive responses (**Supplementary Fig. 12**) and the small size

of the 2nd instar larvae limits the resolution of the analysis. To control the temperature, we used a QE-1HC quick exchange heating/cooling platform with a CL-100 bipolar temperature controller (Warner Instruments, Hamden, CT, USA). To facilitate rapid temperature changes during the heating and cooling, we reduced the buffer volume using an apparatus consisting of a copper chamber (1-5/8" in diameter, 1/16" thick and included ¼" glass windows on the bottom), which fit the QE-1HC. We dissected larvae in 35 mm Petri dishes containing HL-6 buffer (2 mM Ca^{2+}, 340 Osm, pH of 7.2, 7 mM L-glutamic acid), which is the same buffer for Ca^{2+} imaging, and quickly placed the larval brain in the center of the copper chamber. To determine the temperatures that the larvae were exposed to during the experiments, we placed a temperature probe directly adjacent to the larval brain in the center of the copper chamber. In order to accurately control the position of the temperature probe, we designed and made the probe holder by 3D printing, which can be ordered from https://www.shapeways.com/product/SJWE7RXVX/temperature-probe-holder-for-ca2-imaging?key=dbcb76f34fa91de50fe5c9110304efab. We exposed each brain to only one temperature ramp.

We performed the Ca^{2+} imaging using an upright Zeiss LSM700 Confocal Laser Scanning Microscopy, a 20x/1.0 Plan-Apochromat water immersion objective, and Zen software. The wavelength of the laser used for exciting the GCaMP6f was 488 nm. The frame rate of the scanning was 2.2 frames per second. The increase in Ca^{2+} level in each neuron was indicated by $\Delta F/F_0$, where the F_0 was the average baseline fluorescence during the first 90 seconds of the experiment before the temperature

was increased. ΔF was the fluorescence change relative to F_0. To determine the $\Delta F/F_0$, we used the Bio-formats toolbox (http://loci.wisc.edu/software/bio-formats) and MATLAB. Photobleaching decreases the fluorescence according to the following relation: $F = F_0\exp(-kt)$. Therefore, in the absence of any temperature change, the formula is: $\Delta F/F_0 = (F - F_0)/F_0 = \exp(-kt) - 1$. To obtain the photobleaching factor k, we fit the $\Delta F/F_0$ curve before and after the temperature stimuli according to the preceding equation, and then used factor k to compensate for photo-bleaching: $(\Delta F/F_0)_{corrected} = ((\Delta F/F_0)_{measured} + 1)\exp(kt) - 1$. After making this correction, the $\Delta F/F_0$ before and after heat treatment were the same.

Two-electrode recordings in Xenopus oocytes

We recorded TRPA1 currents in *Xenopus laevis* oocytes as we described previously [29]. We maintained the *Xenopus laevis* females (Xenopus 1 Inc.) at ~19 °C under 12 hour light/dark cycle. The ovaries were taken from the female *Xenopus* by surgery and treated with 2 mg/ml collagenase A (Roche) in OR2 Ringers (100 mM NaCl, 2 mM KCl, 1 mM $MgCl_2$, 5 mM HEPES, pH 7.5). We checked the status of the oocytes every 15 min to ensure that the oocytes were completely deflocculated. We cultured the oocytes at 15-19 °C for 12 hours to let them recover in OR3 medium: 50% Leibovits's media L-15 (Sigma L1518), 13 mM HEPES, 90 μg/mL gentamicin, 90 μg/ml Fungizone (Amphotericin B), 90 μg/ml penicillin/streptomycin (pH 7.5).

We linearized the *pOX-trpA1-A* [28], *pOX-trpA1-D* [14], and *pCS2-rTRPV1* constructs overnight and generated *trpA1-A* mRNA using the mMessage mMachine

kit (Ambion). We injected the stage V-VI oocytes with 50 nl *trpA1-A* mRNA (1 μg/μl unless indicated otherwise) or water, and incubated the oocytes at 18 °C for 3 days before performing the two-electrode voltage clamp experiments.

We used a buffer perfusion system to control the temperature of the oocytes. The system contained a SH-27B in-line heater with a TC-324B temperature controller (Warner Instruments, Hamden, CT, USA), which we controlled with a custom LabView program. The buffer used in the system is ND96 (96 mM NaCl, 1 mM $MgCl_2$, 4 mM KCl, and 5 mM HEPES, pH 7.6). For most experiments (**Fig. 7c,e,f**) we included 1.8 mM $CaCl_2$ in the ND96 buffer. For the experiments in **Fig. 7d**, we added 1 mM EGTA to the ND96 buffer to chelate the Ca^{2+}. We performed the recordings at −40 mV using a TURBO TEC-03X two electrode clamp system and Cellwork software (NPI Electronics, Tamm, Germany). Due to the large currents produced in the absence of Ca^{2+}, we reduced the mRNA injected to the oocytes by to 0.1 μg/μl). To calculate the Q_{10}, we fitted the current-temperature curve with the following equation: $I = I_0 10^{(T - T0)/Q10}$ [44]. For each oocyte, we applied two different temperature ramp to calculate a pair of Q_{10} under different temperature changing rates.

Statistical analyses

To obtain the F_{peak} and T_{middle} parameters from the assays of larval thermal nociception, we applied sigmoid functions ($F_{rolling} = (F_{peak} - F_{baseline})/(1+\exp(-(T-T_{middle})/k)) + F_{baseline}$) to fit the $F_{rolling}$-T curve. For each condition, we repeated the experiments at least three times to obtain sets of F_{peak} and T_{middle} data for the

statistical tests. For the data shown in **Fig. 1j, k**, we performed one-way ANOVA on the F_{peak} and T_{middle} under different temperature changing rates. [F_{peak}: n = 3, 5, 7, 3, 3, 6, 3, 7, 9; $F(8,37) = 9.33$; $p = 6.2 \times 10^{-7}$. T_{middle}: n = 3, 5, 7, 3, 3, 6, 3, 7, 9; $F(8,37) = 10.56$; $p = 1.5 \times 10^{-7}$]. The p values for the ANOVA were one-sided. The variances between groups were verified using the Brown-Forsythe test [F_{peak}: $F(8,37) = 1.49$, $p = 0.20$; T_{middle}: $F(8,37) = 0.49$, $p = 0.86$]. The p value for the Brown-Forsythe test was one-sided. We used the Tukey-Kramer test to ascertain statistically significant differences relative to the fastest temperature changing rate (0.5 °C/s). The conditions with significant differences are indicated by asterisks (* $p < 0.05$, ** $p < 0.01$). The p values for the Tukey-Kramer test were two-sided. Data distribution was assumed to be normal but this was not formally tested. No statistical methods were used to pre-determine sample sizes but our sample sizes are similar to those reported in previous publications [1, 40, 45].

For the data shown in **Supplementary Fig. 3j, k**, we performed one-way ANOVA on the F_{peak} and T_{middle} using the different rates of temperature change. [F_{peak}: n = 3, 3, 6, 3, 3, 3, 4, 3, 5; $F(8,24) = 17.81$; $p = 2.4 \times 10^{-8}$. T_{middle}: n = 3, 3, 6, 3, 3, 3, 4, 3, 5; $F(8,24) = 1.79$; $p = 0.13$]. The p values for the ANOVA were one-sided. The variances between groups were verified using the Brown-Forsythe test [F_{peak}: $F(8,24) = 0.53$, $p = 0.82$; T_{middle}: $F(8,24) = 0.53$, $p = 0.82$]. The p value for the Brown-Forsythe test was one-sided. We used the Tukey-Kramer test to ascertain statistically significant differences relative to the fastest temperature changing rate (0.5 °C/s). The conditions with significant differences are indicated by asterisks (* $p < 0.05$, ** $p < 0.01$). The p values for the Tukey-Kramer test were

two-sided. Data distribution was assumed to be normal but this was not formally tested. No statistical methods were used to pre-determine sample sizes but our sample sizes are similar to those reported in previous publications [1, 40, 45].

In **Fig. 4d**, we performed one-way ANOVA on the F_{peak} values for the different genotypes [n = 3, 4, 4, 8, 9, 8, 3, 4, 3; $F(8,37) = 45.38$; $p = 8.1 \times 10^{-17}$]. The p values for the ANOVA were one-sided. The variance similarities between groups were verified using the Brown-Forsythe test [$F(8,37) = 0.21$, $p = 0.99$]. The p value for the Brown-Forsythe test was one-sided. We used the Tukey-Kramer test to determine statistically significant differences between the control (w^{1118}) and other samples. The genotypes with significant differences from the control are indicated with asterisks (*** $p < 0.001$). The p values for the Tukey-Kramer test were two-sided. Data distribution was assumed to be normal but this was not formally tested. No statistical methods were used to pre-determine sample sizes but our sample sizes are similar to those reported in previous publications [1, 40, 45].

To compare the optogenetics data (**Fig. 4e**), we performed the Fisher's exact test between each genotype. The p values for the Fisher's exact test were two-sided. ** $p < 0.01$, *** $p < 0.001$. [Between *UAS-CsChrimson/+* and *UAS-CsChrimson/CyO;trpA1-AB^{GAL4}*: Odds Ratio = 32, $p = 0.00016$; Between *UAS-CsChrimson/+* and *UAS-CsChrimson/tsh-GAL80;trpA1-AB^{GAL4}*: Odds Ratio = 22, $p = 0.0028$; Between *UAS-CsChrimson/CyO;trpA1-AB^{GAL4}* and *UAS-CsChrimson/tsh-GAL80;trpA1-AB^{GAL4}*: Odds Ratio = 0.69, $p = 0.74$.]. No statistical methods were used to pre-determine sample sizes but our sample sizes are similar to those reported in previous publications [20, 36].

To analyze the *in vivo* Ca^{2+} imaging data (**Fig. 6),** we performed one-way ANOVA on the maximum $\Delta F/F_0$ values obtained from BLP neurons during the different temperature changing rates (**b,e,h,k**) [n = 15, 13, 18, 21; $F(3,63) = 13.86$; $p = 4.7 \times 10^{-7}$]. The p values for the ANOVA were one-sided. The variance similarities between groups were verified using the Brown-Forsythe test [$F(3,63) = 6.14$, $p = 9.9 \times 10^{-4}$]. The p values for the Brown-Forsythe test were one-sided. We used the Tukey-Kramer test to ascertain statistically significant differences between two samples [Between (**b**) and (**h**): $q(63,4) = 6.07$; $p = 3.6 \times 10^{-4}$, Between (**b**) and (**k**): $q(63,4) = 8.72$; $p = 3.3 \times 10^{-7}$, Between (**e**) and (**k**): $q(63,4) = 5.10$; $p = 0.034$]. The p values for the Tukey-Kramer test were two-sided. We also performed one-way ANOVA on the maximum $\Delta F/F_0$ values obtained from BLA neurons during the different temperature changing rates (**c,f,i,l**) [n = 10, 11, 6, 6; $F(3,29) = 8.01$; $p = 4.9 \times 10^{-4}$]. The p values for the ANOVA were one-sided. The variance similarities between groups were verified using the Brown-Forsythe test [$F(3,29) = 0.86$, $p = 0.47$]. The p value for the Brown-Forsythe test was one-sided. We used the Tukey-Kramer test to ascertain statistically significant differences between two samples [Between (**c**) and (**i**): $q(29,4) = 3.80$; $p = 0.054$, Between (**c**) and (**l**): $q(29,4) = 6.65$; $p = 3.2 \times 10^{-4}$, Between (**f**) and (**l**): $q(29,4) = 4.85$; $p = 0.0093$]. The p values for the Tukey-Kramer test were two-sided. Data distribution was assumed to be normal but this was not formally tested. No statistical methods were used to pre-determine sample sizes but our sample sizes are similar to those reported in previous publications [22, 45, 46].

To obtain the Q_{10} for each temperature ramp (0.05 °C/s and 0.2 °C/s; **Fig. 7e-f**), we fitted the current-temperature curve with the following equation: $I = I_0 10^{(T - T0)/Q10}$ [44]. We compared the Q_{10} corresponding to the slow temperature ramps and fast temperature ramps using the Wilcoxon signed rank test, which is a nonparametric test for two populations when the observations are paired. This nonparametric test is not based on the assumption that the means of the Q_{10} differences follow normal distributions. The results in **Fig. 7c,e,f** indicated that the Q_{10} was significantly larger when the rate of change was 0.2 °C/s relative to 0.05 °C/s (**Fig. 7c**: $n = 15$, $W = 120$, $p = 6.1 \times 10^{-5}$; **Fig. 7e**: $n = 12$, $W = 54$, $p = 0.034$; **Fig. 8f**: $n = 10$, $W = 47$, $p = 0.014$). The results in **Fig. 7d** indicated that the Q_{10} was not significantly different when the rate of change was 0.2 °C/s versus 0.05 °C/s ($n = 18$, $W = 65$, $p = 0.16$). The p value for the Wilcoxon signed rank test was two-sided. We also used the Wilcoxon signed rank test to compare the total current during the slow and fast temperature ramps (**Supplementary Fig. 10**; $n = 15$, $W = 120$, $p = 6.1 \times 10^{-5}$). No statistical methods were used to pre-determine sample sizes but our sample sizes are similar to those reported in previous publications [14, 28, 47].

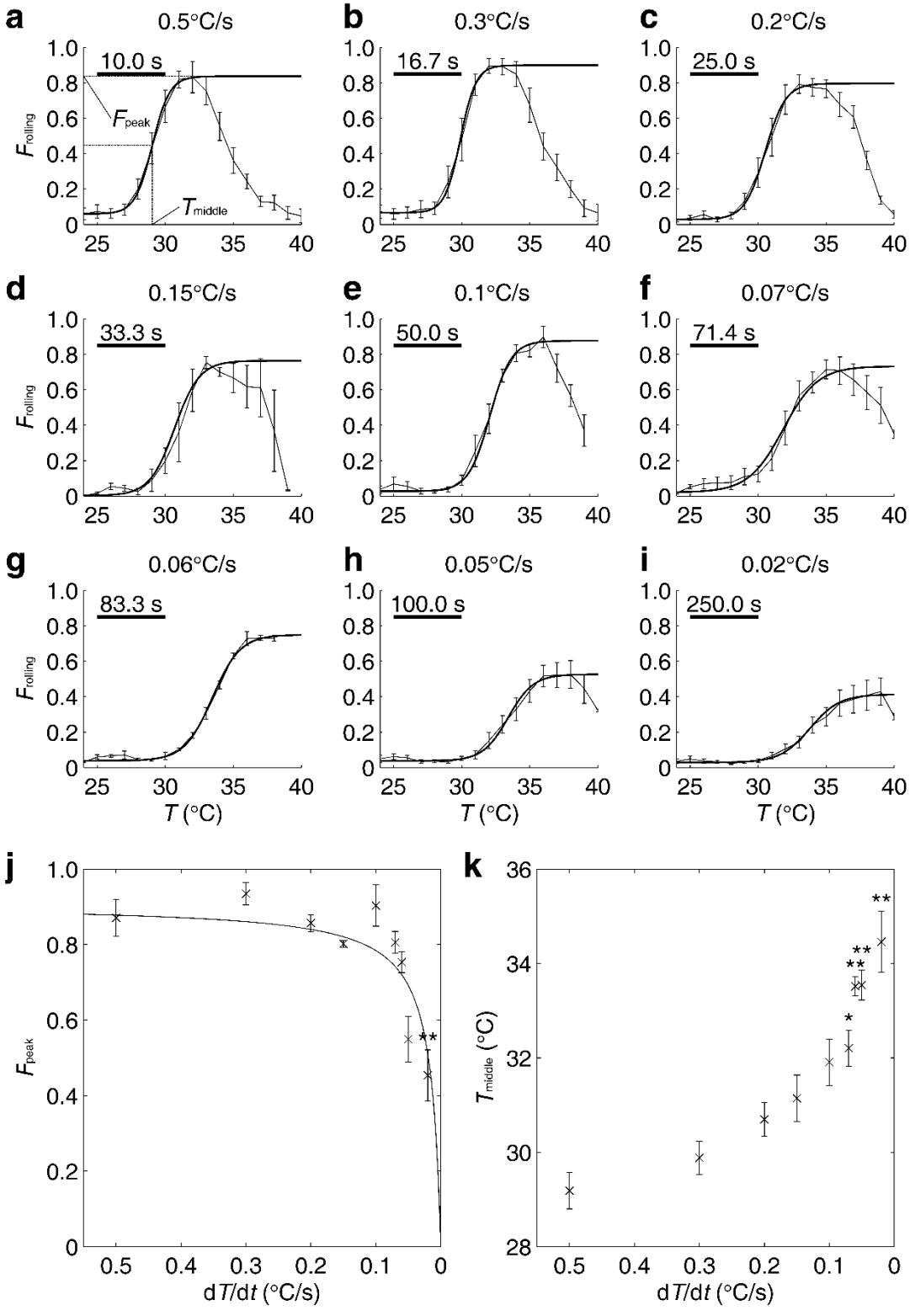
a
0.5°C/s
10.0 s
F_{peak}
T_{middle}
b
0.3°C/s
16.7 s
c
0.2°C/s
25.0 s
d
0.15°C/s
33.3 s
e
0.1°C/s
50.0 s
f
0.07°C/s
71.4 s
g
0.06°C/s
83.3 s
h
0.05°C/s
100.0 s
i
0.02°C/s
250.0 s
$F_{rolling}$
T (°C)
j
F_{peak}
dT/dt (°C/s)
k
T_{middle} (°C)
dT/dt (°C/s)

Figure 1. Rolling responses of wild-type larvae exposed to different rates of temperature increase. (**a-i**) The fraction of control (w^{1118}) 2nd instar larvae that rolled ($F_{rolling}$) as a function of the rate of temperature change (dT/dt, indicated above each plot). The scale bars indicate the seconds required for the temperature to rise by 5 °C. $F_{rolling}$ was defined as $N_{rolling}/N_{total}$, where $N_{rolling}$ was the number of larvae rolling and N_{total} was the total number of larvae. F_{peak} was the maximum rolling fraction and T_{middle} was the temperature corresponding to the point when the rolling fraction rose to half the F_{peak}. The curves (thicker lines) were fit using a sigmoid function. Total number of larvae per experiment ≥30. Number of experiments n = 3, 5, 7, 3, 3, 6, 3, 7, 9 in **a-i**, respectively. (**j**) F_{peak} values as a function of dT/dt. The crosses indicate the average F_{peak} values in response to the different temperature changing rates. (**k**) T_{middle} values as a function of dT/dt. The crosses indicate the average T_{middle} values. We performed one-way ANOVA on the F_{peak} and T_{middle} obtained during the different temperature changing rates [F_{peak}, $F(8,37) = 9.33$, p = 6.2 x 10^{-7}; T_{middle}, $F(8,37) = 10.56$, p = 1.5 x 10^{-7}]. We used the Tukey-Kramer test to ascertain statistically significant differences relative to the fastest temperature changing rate (0.5 °C/s). The following are significant differences: 1) 0.5 °C/s vs 0.02 °C/s: F_{peak}, $q(37,9) = 6.47$, p=0.0016; T_{middle}, $q(37,9) = 8.75$, p = 1.2 x 10^{-5}, 2) 0.5 °C/s vs 0.05 °C/s: T_{middle}, $q(37,9) = 7.30$, p = 0.00027, 3) 0.5 °C/s vs 0.06 °C/s: T_{middle}, $q(37,9) = 6.07$, p = 0.0035 and 4) 0.5 °C/s vs 0.07 °C/s: T_{middle}, $q(37,9)$ = 4.90; p = 0.033. * $p < 0.05$, ** $p < 0.01$. The error bars indicate S.E.M.s.

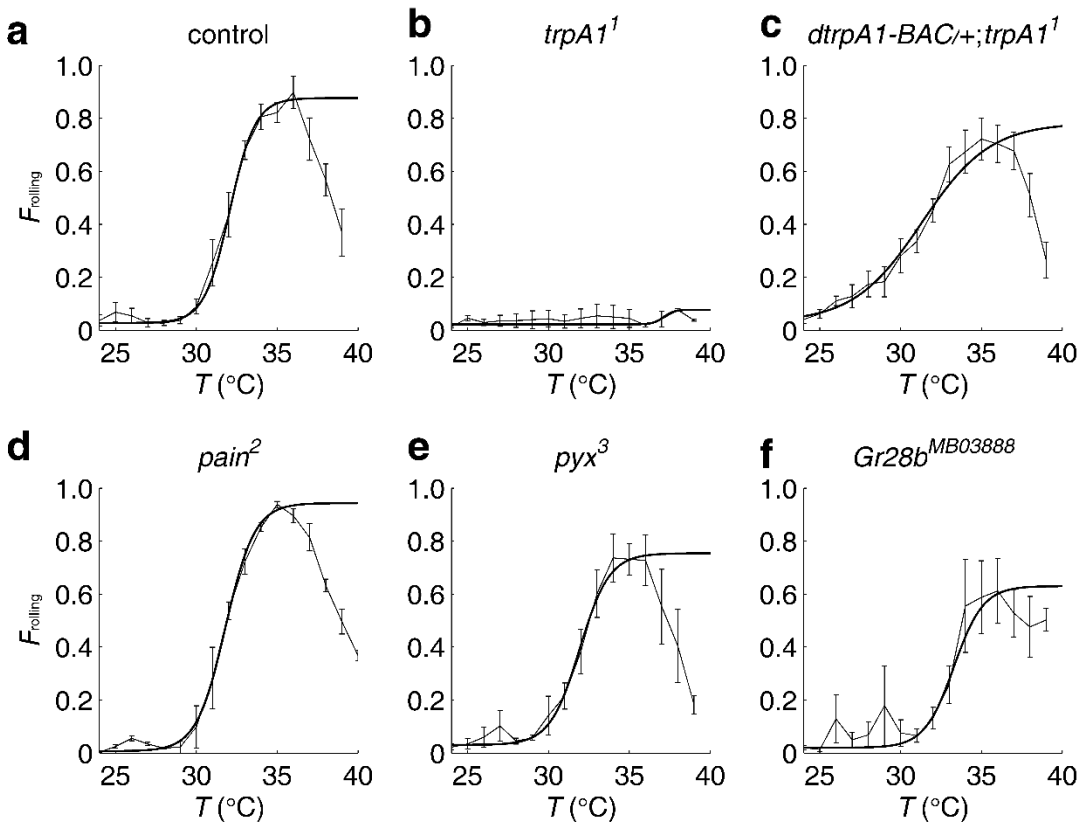

Figure 2. Effects of eliminating different thermoTRPs on $F_{rolling}$ values in response to the same dT/dt. $F_{rolling}$ values exhibited by 2nd instar larvae of the indicated genotypes. dT/dt = 0.1 °C/s. The control larvae in **a** were w^{1118}. Total number of larvae per experiment ≥30. Number of experiments n = 3, 4, 5, 3, 3, 4 in **a-f**, respectively. The error bars indicate S.E.M.s.

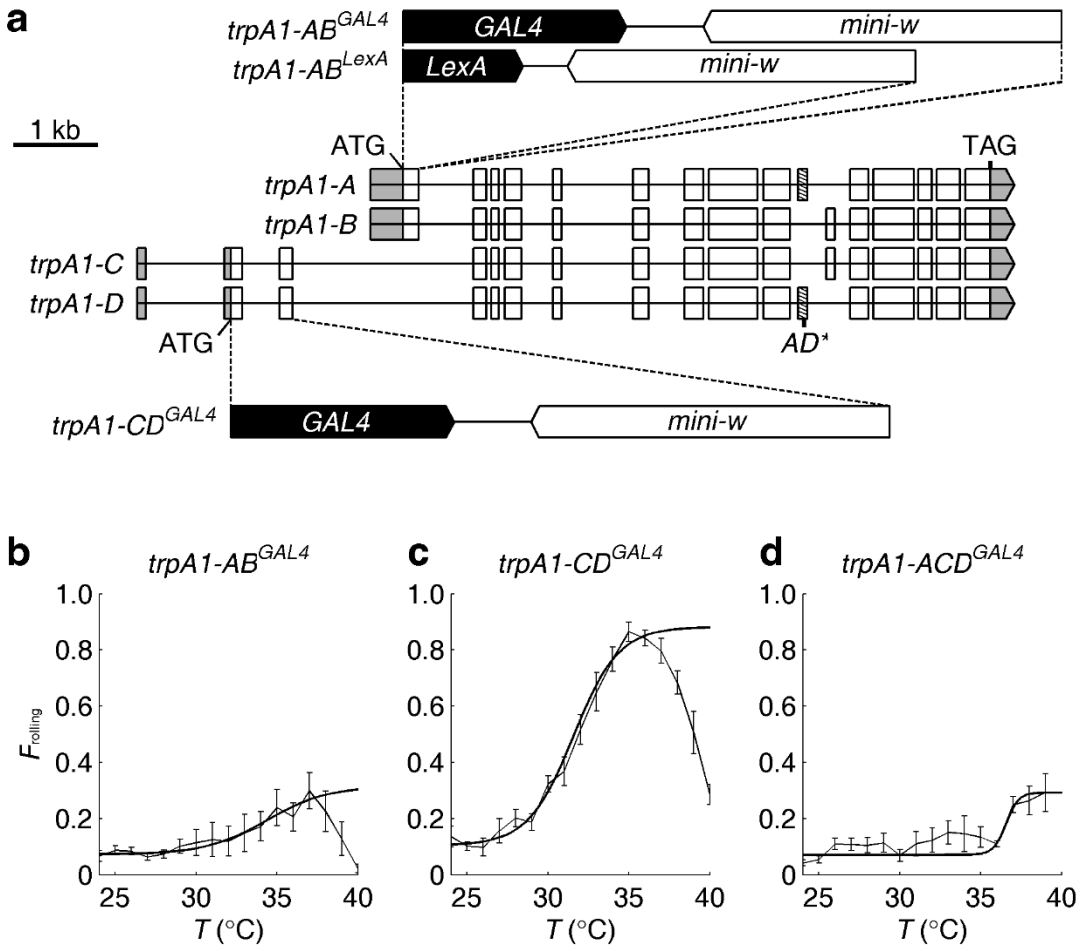

Figure 3. Effects of eliminating different TRPA1 isoforms on F_{rolling} values in response to dT/dt. (**a**) Cartoon depicting the intron-exon organization of the four isoforms encoded by *trpA1*. The structures of the *trpA1* alleles are also indicated. *trpA1-AB*^{GAL4} and *trpA1-AB*^{LexA} both contain a deletion of 178 nucleotides spanning the *trpA1-AB* translation initiation codon and *trpA1-CD*^{GAL4} contains a 732 nucleotide deletion spanning the *trpA1-CD* translation initiation codon. To create flies that expressed only the *trpA1-B* isoform *(trpA1-ACD*^{GAL4}), we introduced a two-nucleotide deletion in the exon common to *trpA1-A* and *trpA1-D* (boxes with diagonal lines) in the *trpA1-CD*^{GAL4} background. The 5' and 3' untranslated regions are indicated in gray. (**b-d**) F_{rolling} values exhibited by 2nd instar larvae of the

indicated genotypes. dT/dt = 0.1 °C/s. Total number of larvae per experiment ≥30. Number of experiments n = 4, 5, 3 in **b-d**, respectively. The error bars indicate S.E.M.s.

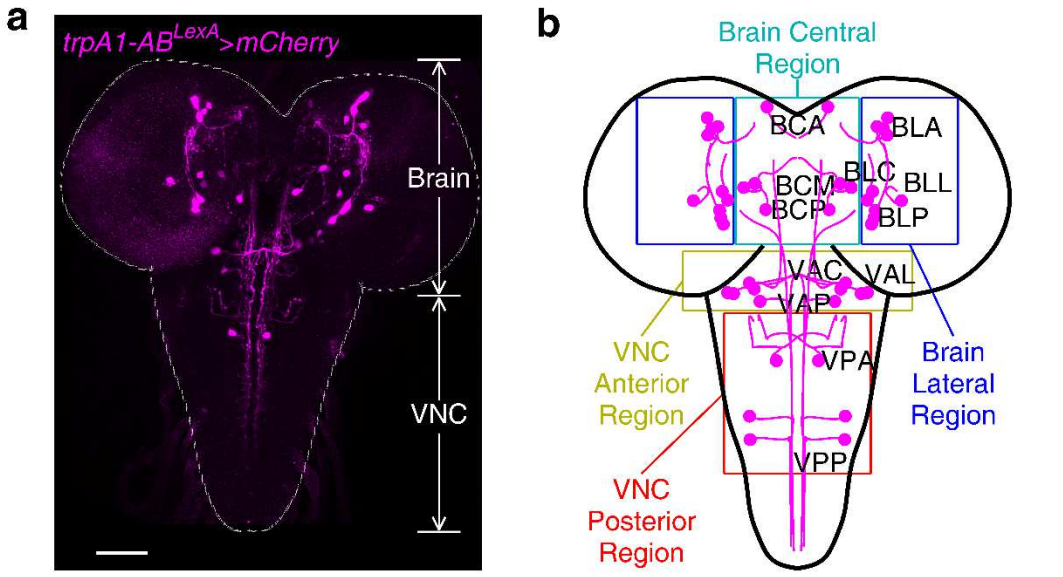

c

	BCA	BCM	BCP	BLA	BLC	BLL	BLP	VAC	VAL	VAP	VPA	VPP
tsh-GAL80;trpA1-AB^{GAL4}							+					
R60F07-GAL4					+		+				+	
386Y-GAL4		+	+	+			+		+			
R21E09-GAL4								+	+			
R21G01-GAL4				+								
R21F01-GAL4		+										

A, anterior; B, brain; C, central; L, lateral; M, medial; P, posterior; V, VNC

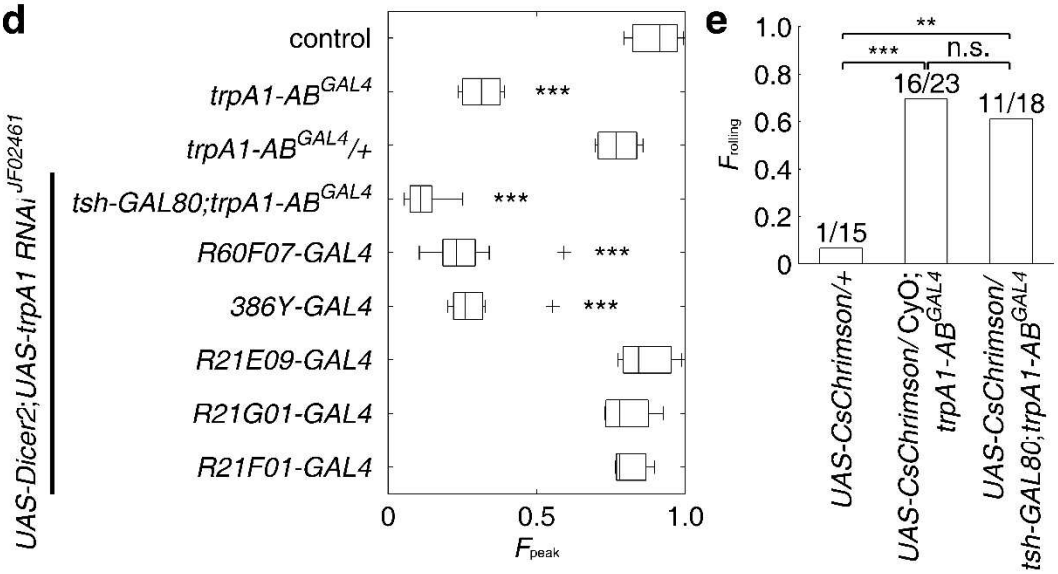

Figure 4. Identifying *trpA1-AB* neurons in the larval brain required for heat-induced rolling. (**a**) Expression of the *trpA1-AB* reporter in the CNS of 3rd instar larvae. The fly line used for the immunostaining with anti-DsRed was *trpA1-AB^{LexA},LexAop-frt-mCherry-STOP-frt-ReaChR::Citrine/+*. The *trpA1-AB* isoforms were expressed in the brain and ventral nerve cord (VNC). The dashed line outlines the brain and VNC. The scale bar represents 50 μm. (n = 7). (**b**) Map of *trpA1-AB* neuronal clusters in the brain and VNC. The colored boxes show the regions that define the first two letters of the three letter nomenclature. The first letter indicates whether the neurons were in the brain (B) or the VNC (V). The second letter indicates the general region within the brain or VNC that contained the neuronal cell bodies: A, anterior; C, central; L, lateral; P, posterior. The third letter indicates the relative positions of the neuronal clusters within the general regions of the brain and VNC: A, anterior; C, central; L, lateral; M, medial, P, posterior. For example, "BLP" indicates the posterior neuronal cluster in the lateral region of the brain. (**c**) Summary of the expression patterns of the indicated *GAL4* reporters in *trpA1-AB* positive neurons of 3rd instar larvae. "+" denotes expression in the indicated neurons. The expression patterns are shown in **Supplementary Figs. 6** and **7**. (**d**) Effect on rolling behavior (F_{Peak}) of 2nd instar larvae resulting from knockdown of *trpA1*, using the *UAS-Dicer2*;*UAS-trpA1 RNAi* line and the indicated *GAL4* drivers. The temperature increased from 23.5 °C to 40 °C with a dT/dt = 0.1 °C/s. The center lines of the boxes represent the median value. The left and right edges of the boxes represent the 25th percentiles ($q_{25\%}$) and 75th percentiles ($q_{75\%}$) of the sample data, respectively. The "+" indicate points as outliers if they are greater than $q_{75\%}$ + 1.5

($q_{75\%} - q_{25\%}$) or less than $q_{25\%} - 1.5$ ($q_{75\%} - q_{25\%}$). The whiskers indicate the minimum and maximum value of data points except for outliers. We performed one-way ANOVA on the F_{peak} values to test for significant different distributions between genotypes [n = 3, 4, 4, 8, 9, 8, 3, 4, 3. The n represents the number of independent experiments. $F(8,37) = 45.38$; $p = 8.1 \times 10^{-17}$]. We used the Tukey-Kramer test to ascertain statistically significant differences between the control (w^{1118}) and other samples. Significant differences relative to the control are indicated (*** $p < 0.001$): 1) *trpA1-AB*^{GAL4}, $q(37,9) = 10.45$, $p = 3.9 \times 10^{-7}$, 2) *UAS-Dicer2*;*UAS-trpA1-RNAi*^{JF02461} X *tsh-GAL80*;*trpA1-AB*^{GAL4}: $q(37,9) = 15.68$, $p = 9.0 \times 10^{-8}$, 3) *UAS-Dicer2*;*UAS-trpA1-RNAi*^{JF02461} X *R60F07-GAL4*: $q(37,9) = 13.12$, $p = 9.1 \times 10^{-8}$, and 4) *UAS-Dicer2*;*UAS-trpA1-RNAi*^{JF02461} X *386Y-GAL4*: $q(37,9) = 12.19$, $p = 9.7 \times 10^{-8}$. (**e**) Triggering rolling behavior of 2rd instar larvae by optogenetically activating *trpA1-AB* neurons. We manually recognized the rolling behaviors of each larvae. We stimulated the larvae with light and scored the larvae with either 1.0 or 0 depending on whether or the not the larvae rolled. The bar heights provide the fraction of larvae that showed rolling behavior. The numbers above the bars are $N_{rolling}/N_{total}$, where $N_{rolling}$ represents the number of larvae rolling and N_{total} provides the total number of larvae. We performed Fisher's exact test between each genotype. We obtained the following values for the following comparisons: 1) *UAS-CsChrimson/+* vs *UAS-CsChrimson*/CyO;*trpA1-AB*^{GAL4} (odds ratio = 32, p = 0.00016), 2) *UAS-CsChrimson/+* vs *UAS-CsChrimson*/*tsh-GAL80*;*trpA1-AB*^{GAL4} (odds ratio = 22, p = 0.0028), 3) *UAS-*

CsChrimson/CyO;*trpA1-AB*^{GAL4} vs *UAS-CsChrimson*/*tsh-GAL80*;*trpA1-AB*^{GAL4} (odds ratio = 0.69, $p = 0.74$). ** $p < 0.01$, *** $p < 0.00$;. n.s., not significant.

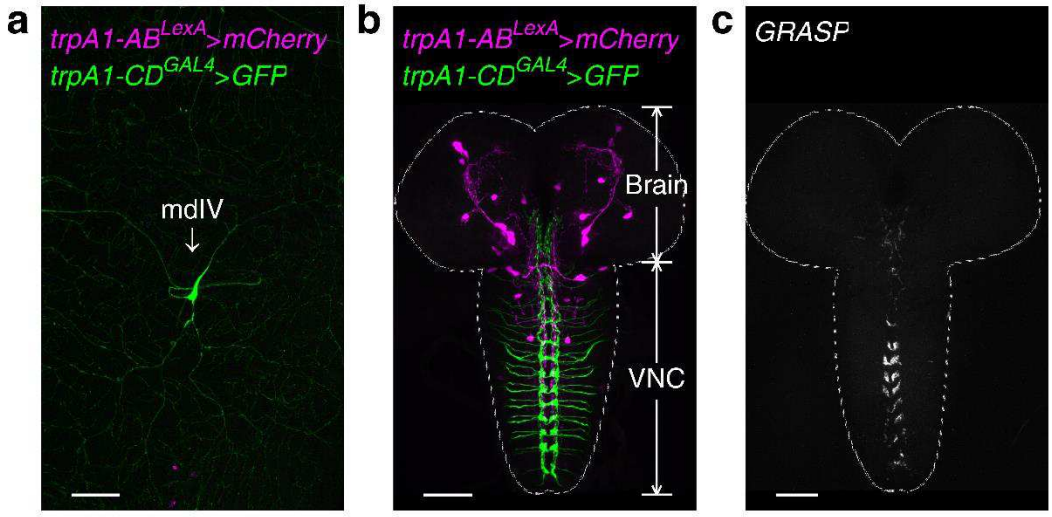

Figure 5. Relative expression of *trpA1-AB* and *trpA1-CD* in the body wall and CNS of 3rd instar larvae. (**a,b**) The fly line used was *UAS-mCD8::GFP/+;trpA1-AB^{LexA},LexAop-frt-mCherry-STOP-frt-ReaChR::Citrine/trpA1-CD^{GAL4}*. The tissues were immunostained with anti-DsRed and anti-GFP. (**a**) Testing for expression of the *trpA1-AB* and *trpA1-CD* reporters in the larval body wall. The *trpA1-CD* but not the *trpA1-AB* reporter labeled peripheral neurons (type IV multidendritic neurons; mdIV) near the body wall. (n = 4). (**b**) Testing for expression of the *trpA1-AB* and *trpA1-CD* reporters in the CNS. The *trpA1-AB* isoforms were expressed in the brain and ventral nerve cord (VNC). The *trpA1-CD* neurons near the body wall projected to the VNC. The dashed line outlines the brain and VNC. (n = 16). (**c**) Application of the GFP reconstitution across synaptic partners (GRASP) technique to investigate whether the *trpA1-CD* neurons and *trpA1-AB* neurons form synapses, using *LexAop-CD4::spGFP11/+;UAS-CD4::spGFP1-10,trpA1-AB^{LexA}/trpA1-CD^{GAL4}*. (n = 3). The scale bars represent 50 μm.

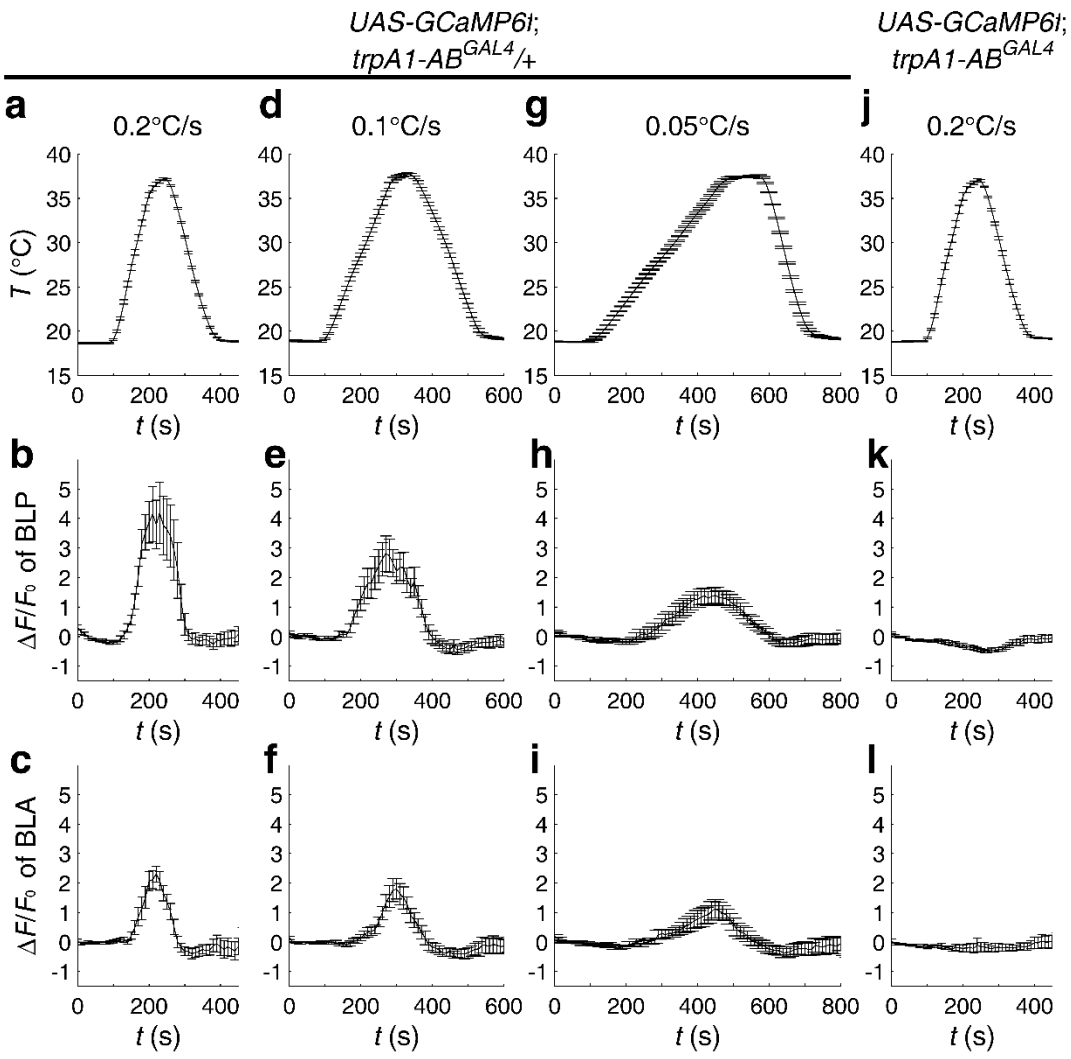

Figure 6. Effects of the rate of temperature change (d*T*/d*t*) on the activities of BLP and BLA neurons of 3rd instar larvae. To assay the activities of BLP and BLA neurons in response to different d*T*/d*t*, we expressed the Ca^{2+} sensor, *UAS-GCaMP6f*, under the control of the *trpA1-AB*^{GAL4} and measured the $\Delta F/F_0$. The d*T*/d*t* are indicated in the top row (**a, d, g, j**). The response profiles of BLP neurons (second row) and BLA neurons (third row) to different d*T*/d*t* are indicated. (**b,c,e,f,h,i**) $\Delta F/F_0$ exhibited by neurons from *trpA1-AB*^{GAL4}/+ heterozygous control brains. (**k,l**) $\Delta F/F_0$ exhibited by neurons from *trpA1-AB*^{GAL4} homozygous mutant

brains. The error bars indicate S.E.M.s. $n \geq 6$. We performed one-way ANOVA on the maximum $\Delta F/F_0$ values of BLP neurons obtained during the different temperature changing rates (**b,e,h,k**) n = 15, 13, 18, 21 in **b,e,h,k**, respectively. [$F(3,63) = 13.86$; $p = 4.7 \times 10^{-7}$]. We used the Tukey-Kramer test to ascertain statistically significant differences between two samples. [**b** vs **h**: $q(63,4) = 6.07$, $p = 3.6 \times 10^{-4}$, **b** vs **k**: $q(63,4) = 8.72$, $p = 3.3 \times 10^{-7}$ and **e** vs **k**: $q(63,4) = 5.10$, $p = 0.034$]. We also performed one-way ANOVA on the maximum $\Delta F/F_0$ values of BLA neurons obtained during the different temperature changing rates (**c,f,i,l**) n = 10, 11, 6, 6 in **c,f,i,l**, respectively. [$F(3,29) = 8.01$; $p = 4.9 \times 10^{-4}$]. We used the Tukey-Kramer test to ascertain statistically significant differences between two samples. [**c** vs **i**: $q(29,4) = 3.80$, $p = 0.054$, **c** vs **l**: $q(29,4) = 6.65$, $p = 3.2 \times 10^{-4}$ and **f** vs **l**: $q(29,4) = 4.85$, $p = 0.0093$].

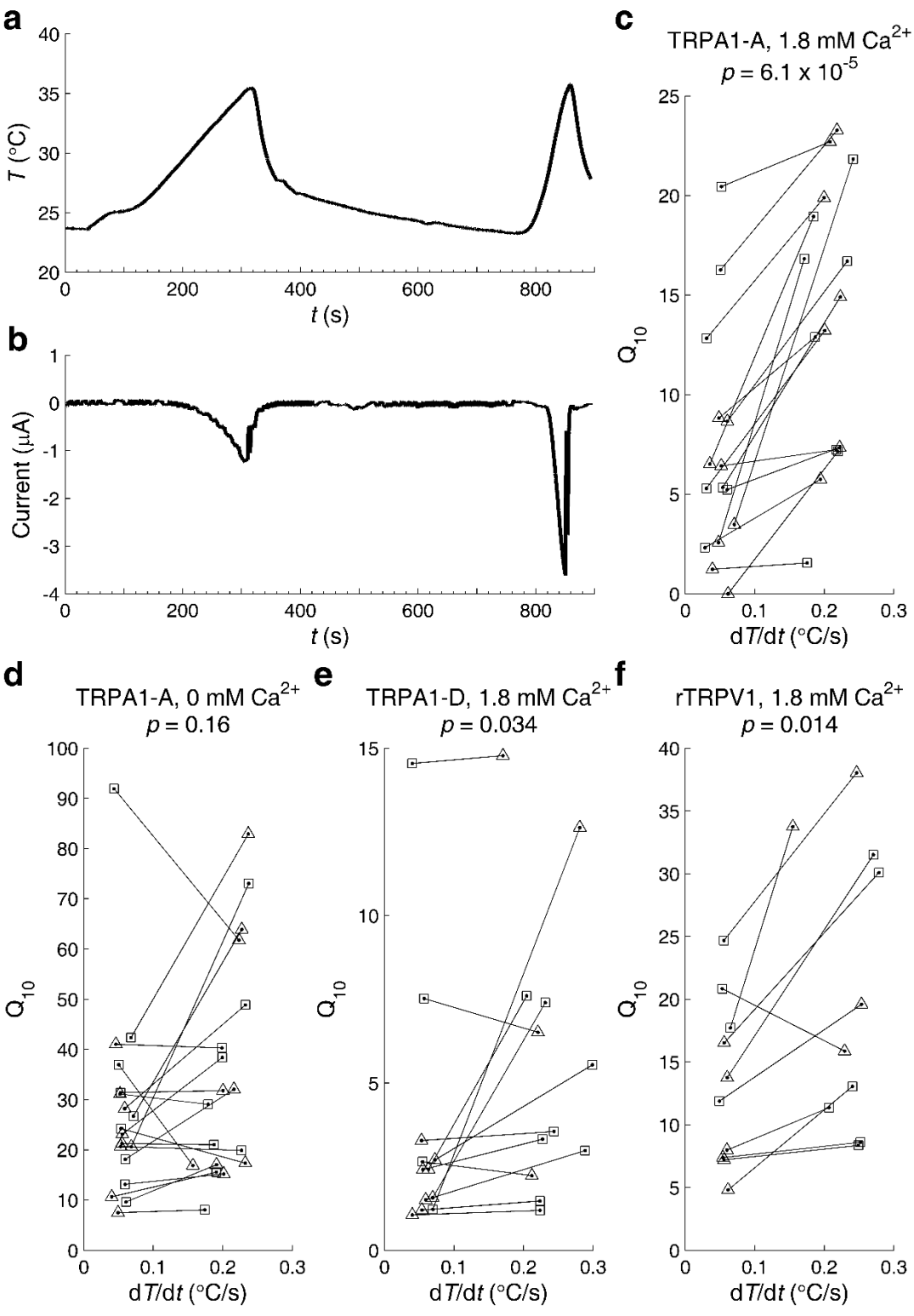
a
T (°C)
t (s)
b
Current (μA)
t (s)
c
TRPA1-A, 1.8 mM Ca2+
p = 6.1 x 10-5
Q10
dT/dt (°C/s)
d
TRPA1-A, 0 mM Ca2+
p = 0.16
Q10
dT/dt (°C/s)
e
TRPA1-D, 1.8 mM Ca2+
p = 0.034
Q10
dT/dt (°C/s)
f
rTRPV1, 1.8 mM Ca2+
p = 0.014
Q10
dT/dt (°C/s)

Figure 7. Effects of the rate of temperature change on the activities of the TRPA1-A and TRPA1-D channels. The indicated channels were expressed in Xenopus oocytes and the currents were recorded during two temperature ramps (d*T*/d*t*: slow, ~0.05 °C/s; fast, ~0.2 °C/s) in ND96 buffer containing either 1.8 mM Ca^{2+} or 1 mM EGTA (0 mM Ca^{2+}) as indicated. (**a**) The oocytes were exposed to two temperature ramps as indicated by the red trace. (**b**) Representative total currents in an oocyte expressing TRPA1-A in the presence of 1.8 mM Ca^{2+} upon exposure a slow and fast d*T*/d*t*. (**c-f**) The indicated TRP channels were expressed in oocytes. The Q_{10} values are shown as a function of d*T*/d*t*. We used linear regression to calculate the temperature changing rates and non-linear curve fitting to calculate the Q_{10} corresponding to the temperature ramp. In each experiment, we treated one oocyte with a slow and a fast temperature ramp. The black lines link the data from the same oocyte. We changed the order of the slow and fast temperature changes so they were similar in number. The squares and triangles indicate the first and second temperature ramp in each experiment, respectively. We compared Q_{10} values corresponding to the slow and fast temperature ramps using the Wilcoxon signed rank test. The *p* values are indicated. (**c**) TRPA1-A currents using a 24 °—35 °C ramp. (n = 15, W = 120, $p = 6.1 \times 10^{-5}$). (**d**) TRPA1-A currents using a 24 °—35 °C ramp. (n = 18, W = 65, p = 0.16). (**e**) TRPA1-D currents using a 24 °—40 °C ramp (n = 12, W = 54, p = 0.034). (**f**) Rat TRPV1 (rTRPV1) currents using a 24 °—48 °C ramp (n = 10, W = 47, p = 0.014).

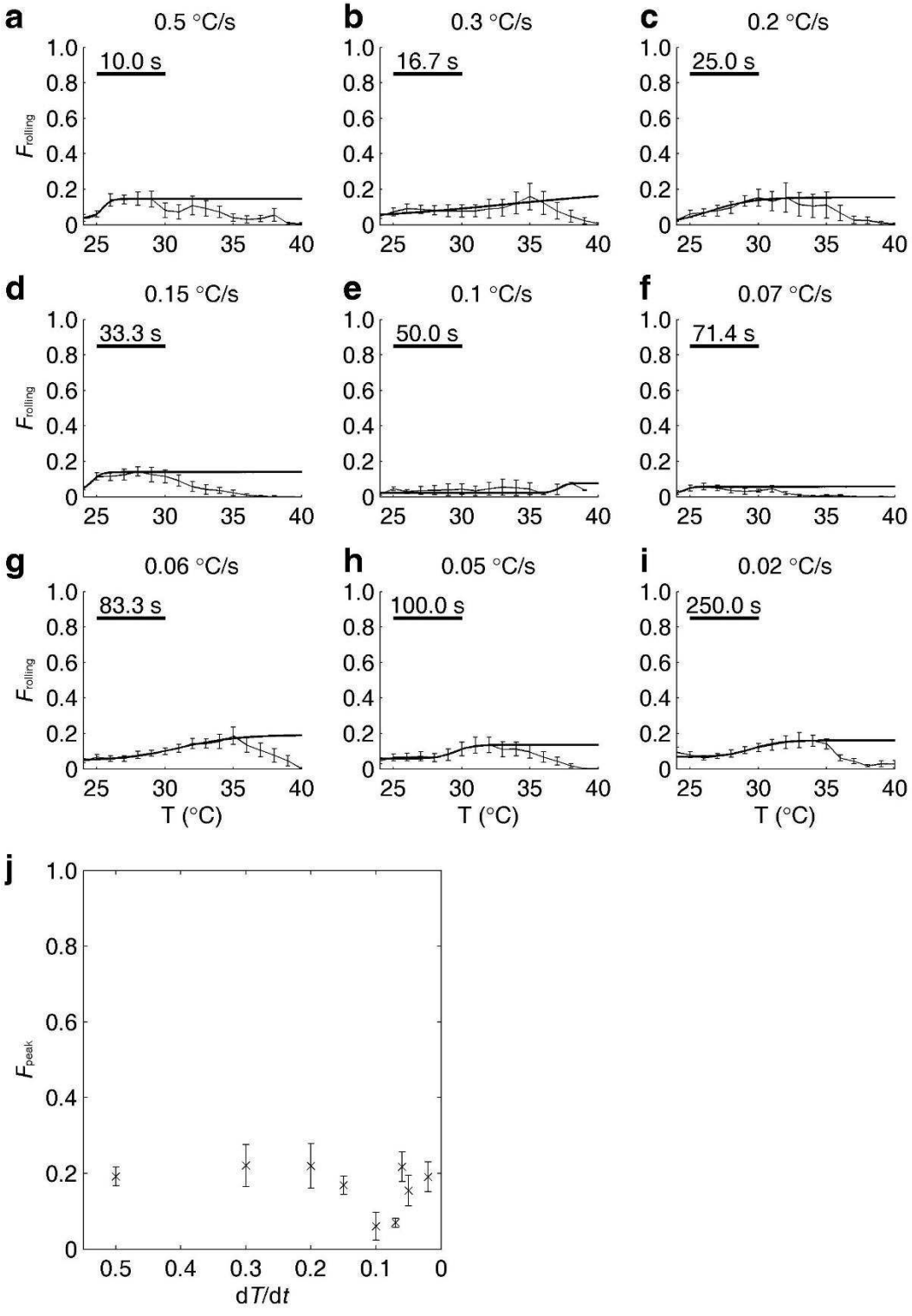
a
0.5 °C/s
10.0 s
b
0.3 °C/s
16.7 s
c
0.2 °C/s
25.0 s
d
0.15 °C/s
33.3 s
e
0.1 °C/s
50.0 s
f
0.07 °C/s
71.4 s
g
0.06 °C/s
83.3 s
h
0.05 °C/s
100.0 s
i
0.02 °C/s
250.0 s
F rolling
T (°C)
j
F peak
dT/dt

Supplementary Figure 1. Rolling responses of *trpA1*^{1} larvae exposed to different rates of temperature increase. (**a-i**) The fraction of *trpA1*^{1} second-instar larvae that rolled ($F_{rolling}$) as a function of the rate of temperature change (dT/dt). The dT/dt are indicated above each plot. The scale bars indicate the seconds required for the temperature to rise by 5 °C. The rolling fraction is defined as $N_{rolling}/N_{total}$, where $N_{rolling}$ is the number of larvae rolling and N_{total} is the total number of larvae. F_{peak} is the maximum rolling fraction and T_{middle} is the temperature corresponding to the point when the rolling fraction rose to half the F_{peak}. The curves (solid black lines) are fit using a sigmoid function. Total number of larvae per experiment ≥ 30; n = 4, 6, 5, 6, 4, 4, 7, 9 and 8 in **a**, **b**, **c**, **d**, **e**, **f**, **g**, **h** and **i**, respectively. (**j**) F_{peak} values as a function of dT/dt. The crosses indicate the average F_{peak} values in response to the different temperature changing rates. Error bars indicate s.e.m.

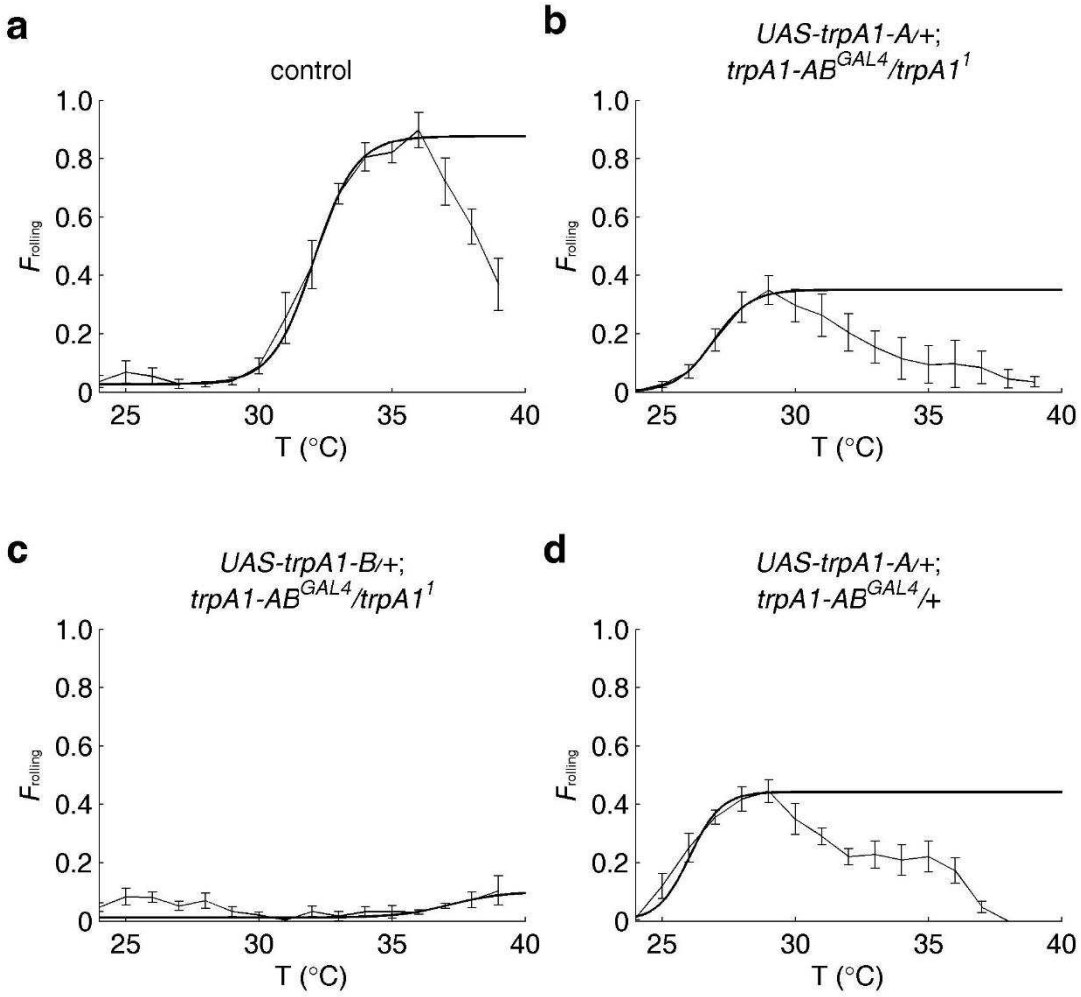

Supplementary Figure 2. Expression of *trpA1-A* using the *GAL4/UAS* system lowered the thermal nociception threshold. Second-instar larvae were exposed to a heat ramp (d*T*/d*t*) of 0.1 °C/s. (**a**) Control (w^{1118}) larvae. n = 3 (≥ 30 larvae per experiment). (**b**) Larvae expressing *trpA1-A* (*UAS-trpA1-A*) using the *trpA1-AB*^{GAL4} in a transheterozygous *trpA1* mutant background (*trpA1*^{1}/*trpA1-AB*^{GAL4}). n = 4 (≥ 30 larvae per experiment). (**c**) Expression of *UAS-trpA1-B* in a *trpA1-AB*^{GAL4}/*trpA1*^{1} background. n = 3 (≥ 30 larvae per experiment). (**d**) Expression of *trpA1-A* (*UAS-trpA1-A*) in a *trpA1-AB*^{GAL4}/+ heterozygous larvae. n = 3 (≥ 30 larvae per experiment).

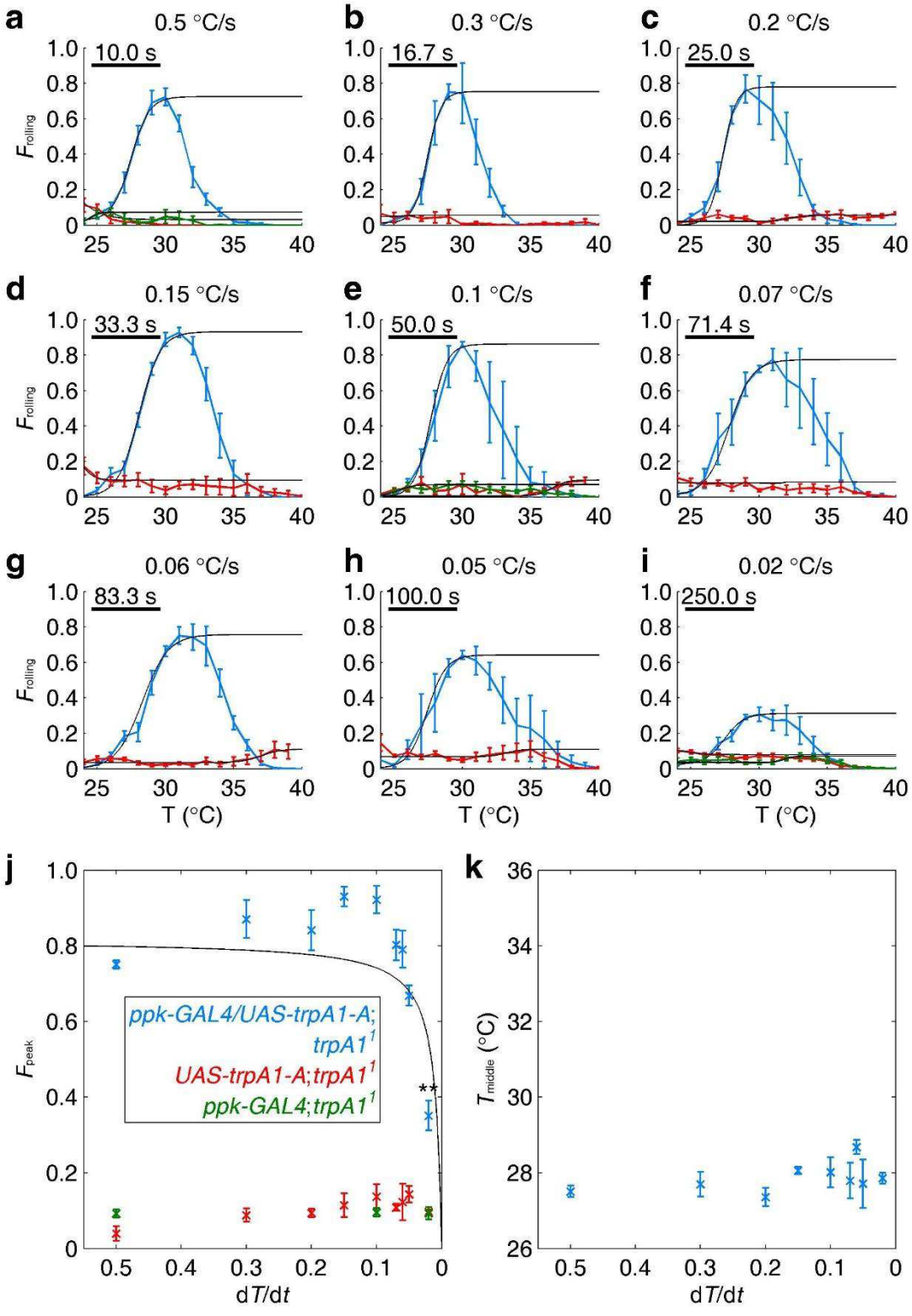
a
0.5 °C/s
10.0 s
b
0.3 °C/s
16.7 s
c
0.2 °C/s
25.0 s
d
0.15 °C/s
33.3 s
e
0.1 °C/s
50.0 s
f
0.07 °C/s
71.4 s
g
0.06 °C/s
83.3 s
h
0.05 °C/s
100.0 s
i
0.02 °C/s
250.0 s
F rolling
T (°C)
j
k
F peak
dT/dt
T middle (°C)
ppk-GAL4/UAS-trpA1-A;
trpA1 1
UAS-trpA1-A;trpA1 1
ppk-GAL4;trpA1 1
**

Supplementary Figure 3. Rolling responses of larvae ectopically expressing *trpA1-A* in mdIV neurons exposed to different rates of temperature increase.

(**a-i**) The fraction of second-instar larvae that rolled ($F_{rolling}$) as a function of the rate of temperature change (dT/dt). Blue, *ppk-GAL4/UAS-trpA1-A*;*trpA1*^{1} (Total number of larvae per experiment ≥ 30; n = 3, 3, 6, 3, 3, 3, 4, 3 and 5 in **a**, **b**, **c**, **d**, **e**, **f**, **g**, **h** and **i**, respectively). Red, *UAS-trpA1-A*;*trpA1*^{1} (Total number of larvae per experiment ≥ 30; n = 4, 3, 5, 3, 3, 3, 4, 3 and 5 in **a**, **b**, **c**, **d**, **e**, **f**, **g**, **h** and **i**, respectively). Green, *ppk-GAL4*;*trpA1*^{1}, only in **a**, **e** and **i** (Total number of larvae per experiment ≥ 30; n = 3, 4 and 4 in **a**, **e** and **i** respectively). The dT/dt are indicated above each plot. The scale bars indicate the seconds required for the temperature to rise by 5 °C. The rolling fraction was defined as $N_{rolling}/N_{total}$, where $N_{rolling}$ was the number of larvae rolling and N_{total} was the total number of larvae. F_{peak} was the maximum rolling fraction and T_{middle} was the temperature corresponding to the point when the rolling fraction rose to half the F_{peak}. The curves (solid black lines) were fit using a sigmoid function. (**j**) F_{peak} values as a function of dT/dt. Crosses, average F_{peak} values in response to the different temperature-change rates. (**k**) T_{middle} values as a function of dT/dt. Crosses, average T_{middle} values. On *ppk-GAL4/UAS-trpA1-A*;*trpA1*^{1}, one-way ANOVA of F_{peak}: $F_{8,24}$ = 17.81; P = 2.4 x 10^{-8}; one-way ANOVA of T_{middle}: $F_{8,24}$ = 1.79; P = 0.13; Tukey-Kramer test for statistically significant differences relative to the highest dT/dt (0.5 °C/s): F_{peak}: 0.5 °C/s vs. 0.02 °C/s: $q_{24,9}$ = 8.77; P = 6.3 x 10^{-5}. *P < 0.05, **P < 0.01; error bars indicate s.e.m.

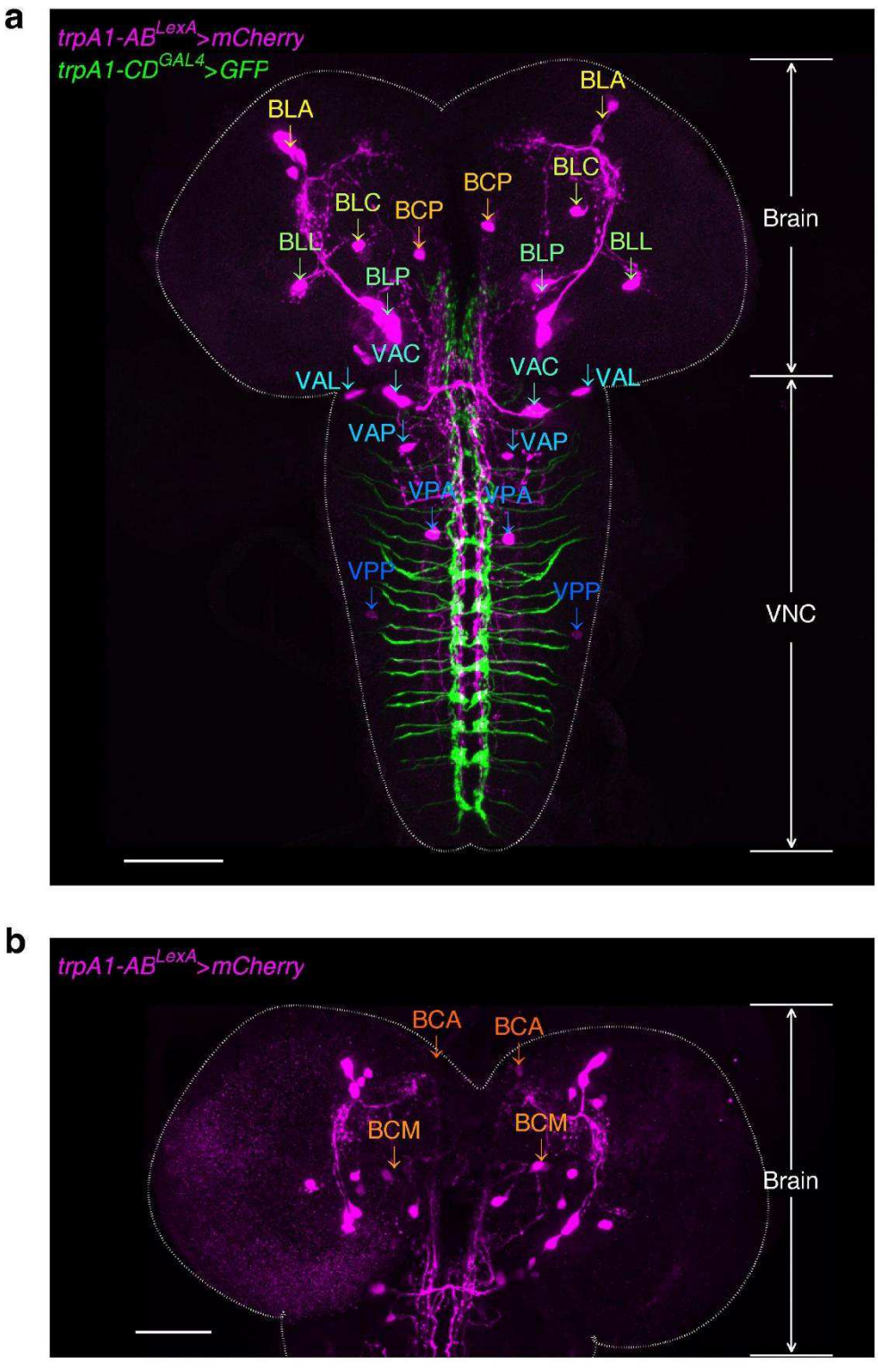
a
trpA1-AB^LexA>mCherry
trpA1-CD^GAL4>GFP
BLA
BLA
BLC
BCP
BLC
BCP
BLL
BLL
BLP
BLP
VAC
VAC
VAL
VAL
VAP
VAP
VPA
VPA
VPP
VPP
Brain
VNC
b
trpA1-AB^LexA>mCherry
BCA
BCA
BCM
BCM
Brain

Supplementary Figure 4. Expression of the *trpA1-AB* and *trpA1-CD* reporters in the CNS of third-instar larvae. (**a**) An enlarged version of **Fig. 5b**. (n = 16). The larval genotype was *UAS-GFP*/+;*trpA1-AB*^{LexA},*LexAop-frt-mCherry-STOP-frt-ReaChR::Citrine/trpA1-CD*^{GAL4}. The colored arrows indicate different *trpA1-AB* neuronal clusters. The first letter indicates whether the neurons were in the brain (B) or the VNC (V). The second letter indicates the general region within the brain or VNC that contained the neuronal cell bodies: A, anterior; C, central; L, lateral; P, posterior. The third letter indicates the relative positions of the neuronal clusters within the general regions of the brain and VNC: A, anterior; C, central; L, lateral; M, medial, P, posterior. The intensities of the BCA, and BCM neurons were not great enough to detect in this image. (**b**) An enlarged version of **Fig. 4a** in which the BCA and BCM neurons were bright enough to detect. (n = 7). The larval genotype was *trpA1-AB*^{LexA},*LexAop-frt-mCherry-STOP-frt-ReaChR::Citrine*/+. Scale bars, 50 μm.

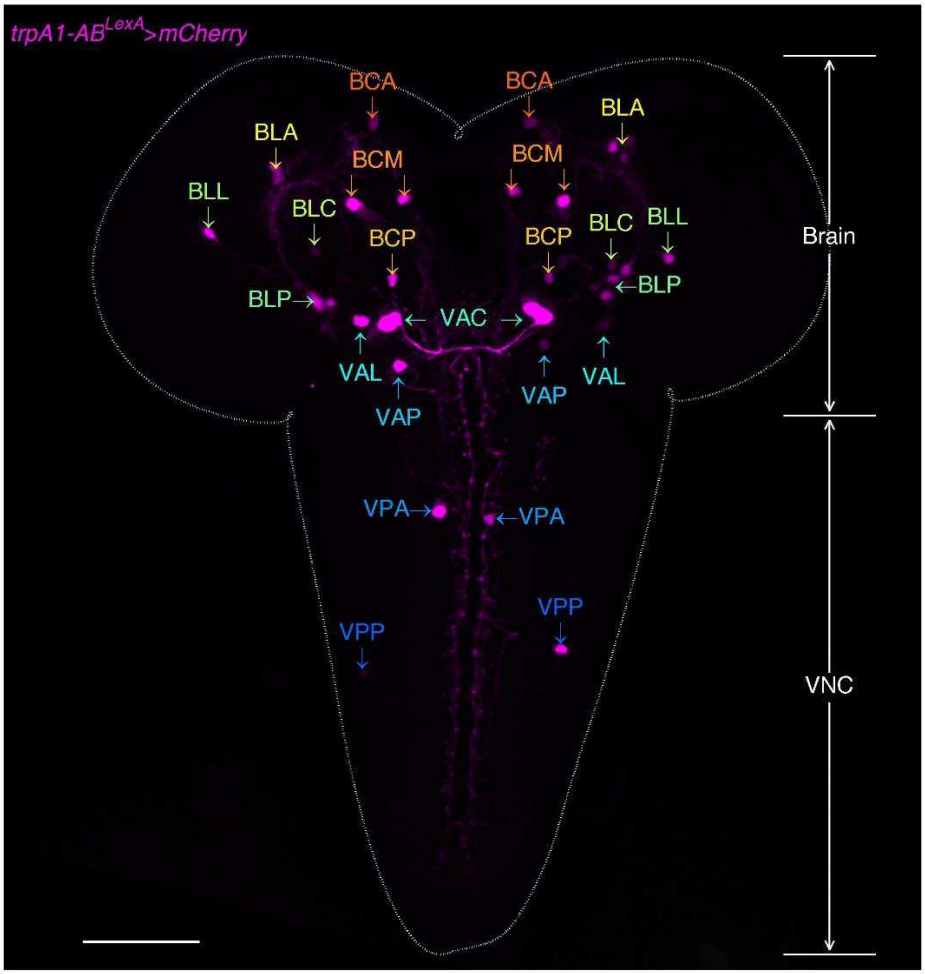

Supplementary Figure 5. Expression of the *trpA1-AB* reporter in the CNS of a *trpA1-AB*^{LexA} homozygous mutant third-instar larva. The colored arrows indicate different *trpA1-AB* neuronal clusters. (n = 9). The larval genotype was *trpA1-AB*^{LexA}*,LexAop-frt-mCherry-STOP-frt-ReaChR::Citrine*. The first letter indicates whether the neurons were in the brain (B) or the VNC (V). The second letter indicates the general region within the brain or VNC that contained the neuronal cell bodies: A, anterior; C, central; L, lateral; P, posterior. The third letter indicates the relative positions of the neuronal clusters within the general regions of the brain and VNC: A, anterior; C, central; L, lateral; M, medial, P, posterior. Scale bars, 50 μm.

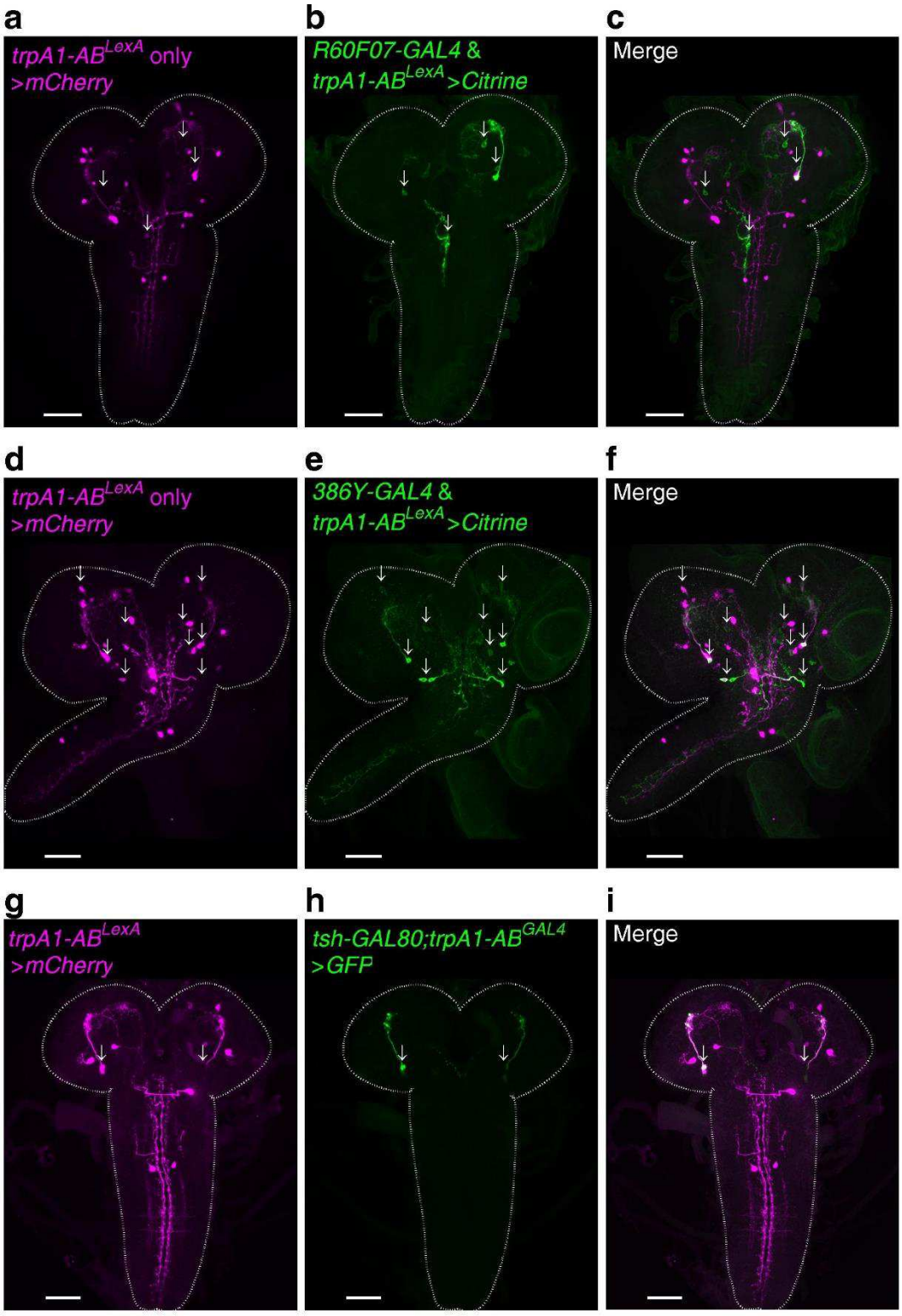
a
trpA1-AB^LexA only
>mCherry
b
R60F07-GAL4 &
trpA1-AB^LexA >Citrine
c
Merge
d
trpA1-AB^LexA only
>mCherry
e
386Y-GAL4 &
trpA1-AB^LexA >Citrine
f
Merge
g
trpA1-AB^LexA
>mCherry
h
tsh-GAL80;trpA1-AB^GAL4
>GFP
i
Merge

Supplementary Figure 6. Overlap of the indicated *GAL4* reporters with the *trpA1-AB*$^{LexA/+}$ reporter in third-instar larvae. The dashed lines outline the larval brain and VNC. The whole mounts were stained with anti-DsRed and anti-GFP. (**a-f**) In addition to the *GAL4* and *trpA1-AB*^{LexA}/+ reporters, the larvae carried *UAS-FLP* and a *LexAop-frt-mCherry-STOP-frt-ReaChR::Citrine* transgenes. (**g-i**) In addition to the *GAL4* and *trpA1-AB*^{LexA}/+ reporters, the larvae carried *UAS-GFP* and a *LexAop-frt-mCherry-STOP-frt-ReaChR::Citrine* transgenes. Scale bars, 50 μm. (*R60F07-GAL4*, $n = 5$; *386Y-GAL4*, $n = 6$; *tsh-GAL80*;*trpA1-AB*^{GAL4}, $n = 5$).

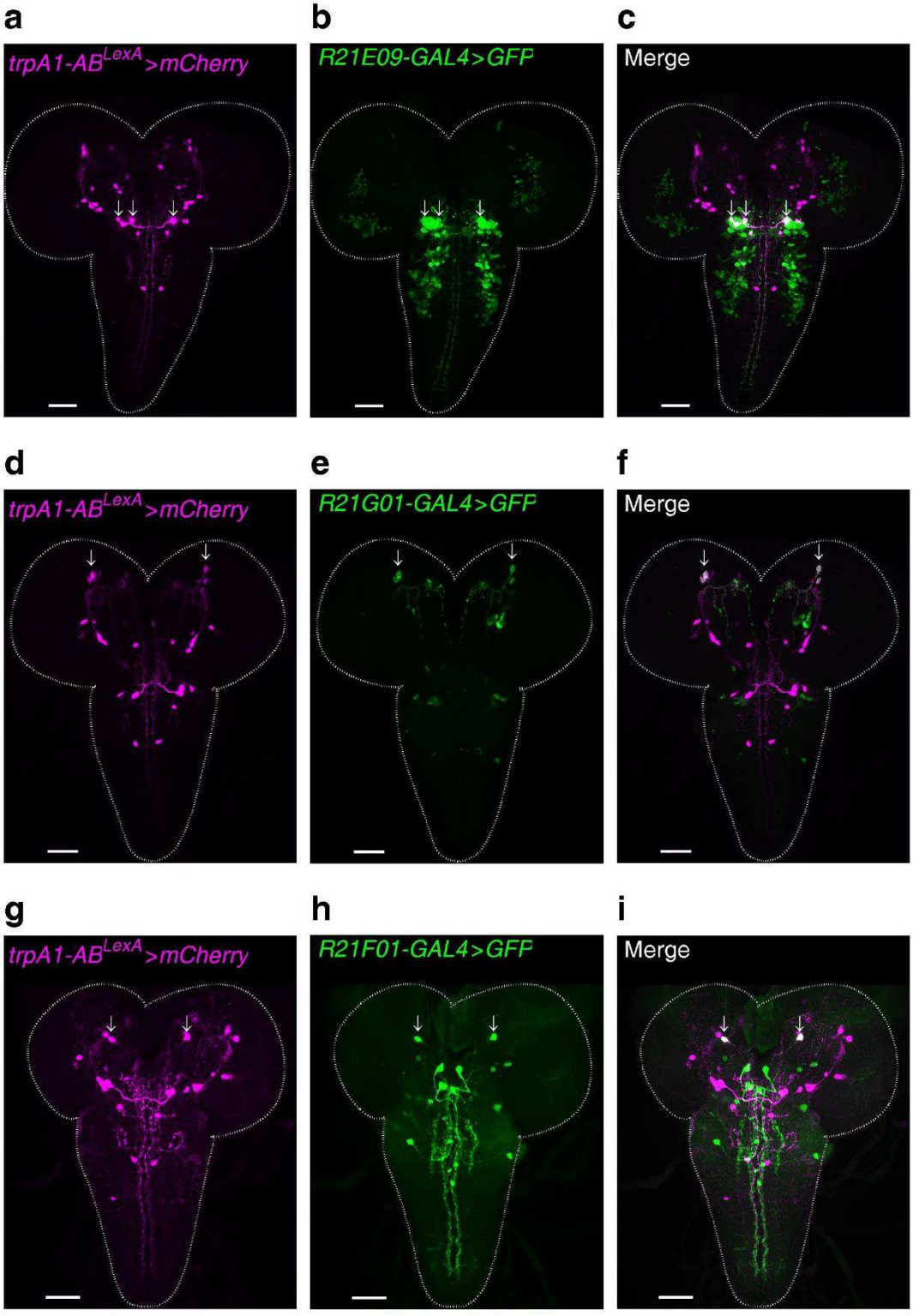
a
trpA1-AB^LexA>mCherry
b
R21E09-GAL4>GFP
c
Merge
d
trpA1-AB^LexA>mCherry
e
R21G01-GAL4>GFF
f
Merge
g
trpA1-AB^LexA>mCherry
h
R21F01-GAL4>GFP
i
Merge

Supplementary Figure 7. Overlap of the indicated *GAL4* reporters with the *trpA1-AB*$^{LexA/+}$ reporter in third-instar larvae. In addition to the *GAL4* and *trpA1-AB*^{LexA}/+ reporters, the flies carried *UAS-GFP* and *LexAop-frt-mCherry-STOP-frt-ReaChR::Citrine* transgenes. The dashed lines outline the larval brain and VNC. The whole mounts were stained with anti-DsRed and anti-GFP. Scale bars, 50 μm. (*R21E09-GAL4*, $n = 4$; *R21G01-GAL4*, $n = 5$; *R21F01-GAL4*, $n = 3$).

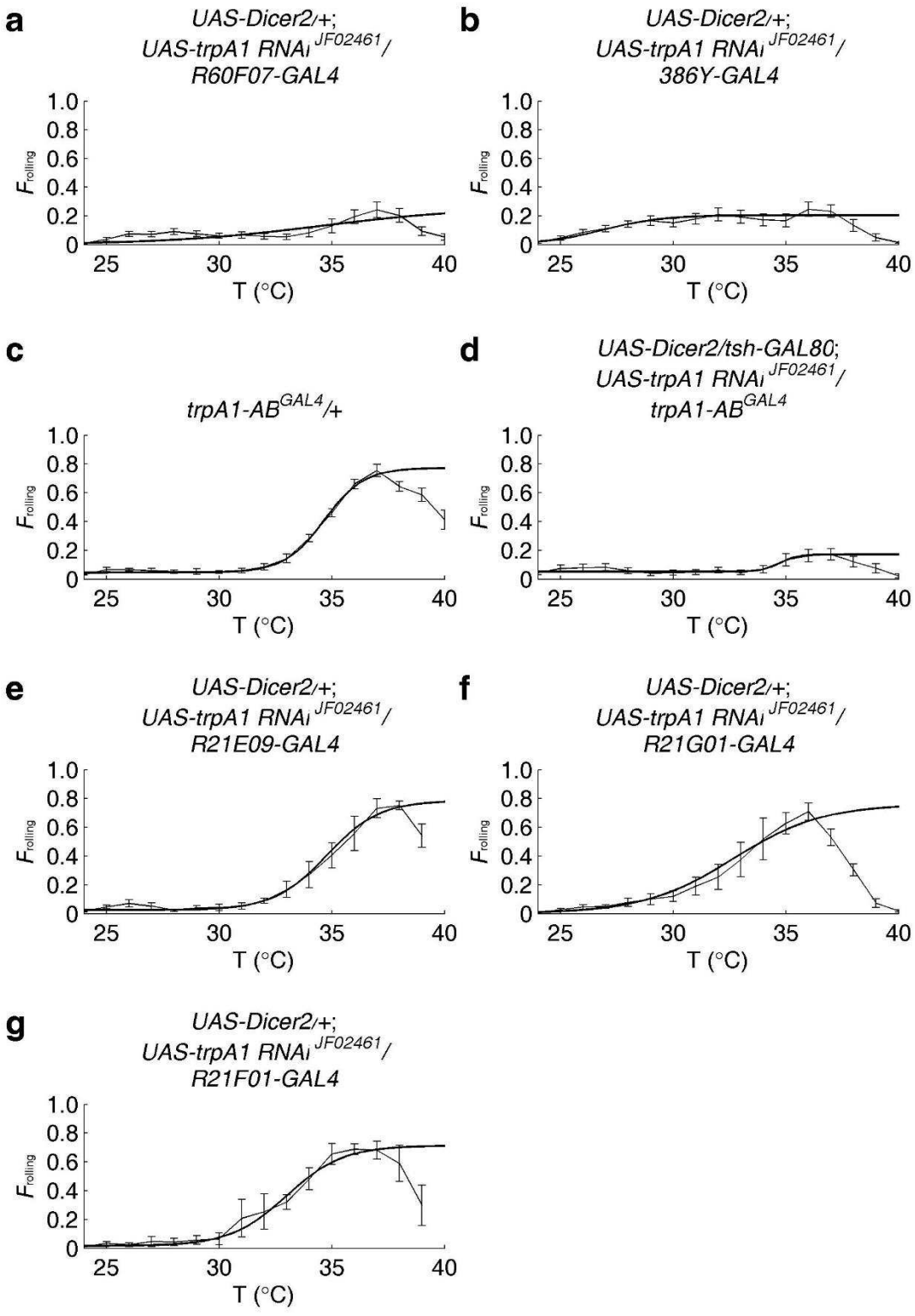
a
UAS-Dicer2/+;
UAS-trpA1 RNAi JF02461/
R60F07-GAL4
b
UAS-Dicer2/+;
UAS-trpA1 RNAi JF02461/
386Y-GAL4
c
trpA1-AB GAL4/+
d
UAS-Dicer2/tsh-GAL80;
UAS-trpA1 RNAi JF02461/
trpA1-AB GAL4
e
UAS-Dicer2/+;
UAS-trpA1 RNAi JF02461/
R21E09-GAL4
f
UAS-Dicer2/+;
UAS-trpA1 RNAi JF02461/
R21G01-GAL4
g
UAS-Dicer2/+;
UAS-trpA1 RNAi JF02461/
R21F01-GAL4
F rolling
T (°C)
0
0.2
0.4
0.6
0.8
1.0
25
30
35
40

Supplementary Figure 8. Effect on rolling behavior (F_{peak}) resulting from knockdown of *trpA1*, using *UAS-Dicer2*;*UAS-trpA1 RNAi* and the indicated *GAL4* drivers. The animals used in these experiments were second-instar larvae. The temperature increased from 23.5 °C to 40 °C with a $dT/dt = 0.1$ °C/s. Total number of larvae per experiment ≥ 30; n = 9, 8, 4, 8, 3, 4 and 3 in **a**, **b**, **c**, **d**, **e**, **f** and **g**, respectively. Error bars indicate s.e.m.

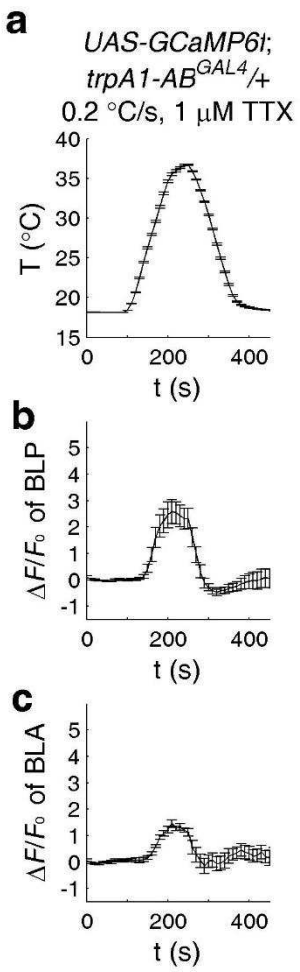

Supplementary Figure 9. The temperature responses of BLP and BLA neurons of third-instar larvae in the presence of tetrodotoxin. In order to address whether the temperature induced responses of BLP and BLA neurons (n = 30 and 9) were caused by presynaptic neurons, we applied 1 μM tetrodotoxin (TTX), which suppresses voltage-gated Na^+ channels and synaptic transmission. These neurons still responded to temperature changes in the presence of TTX.

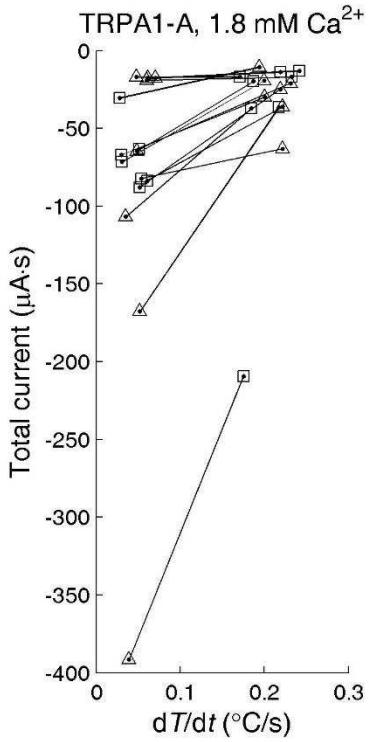

Supplementary Figure 10. Total current under slow and fast ramp conditions in oocytes expressing the TRPA1-A channel. The total current was calculated by integrating the current during the slow and fast heat ramps (the areas under the current curves). We compared the total current under the slow and fast temperature ramps using the Wilcoxon signed rank test: $n = 15$, $W = 120$, $P = 6.1 \times 10^{-5}$).

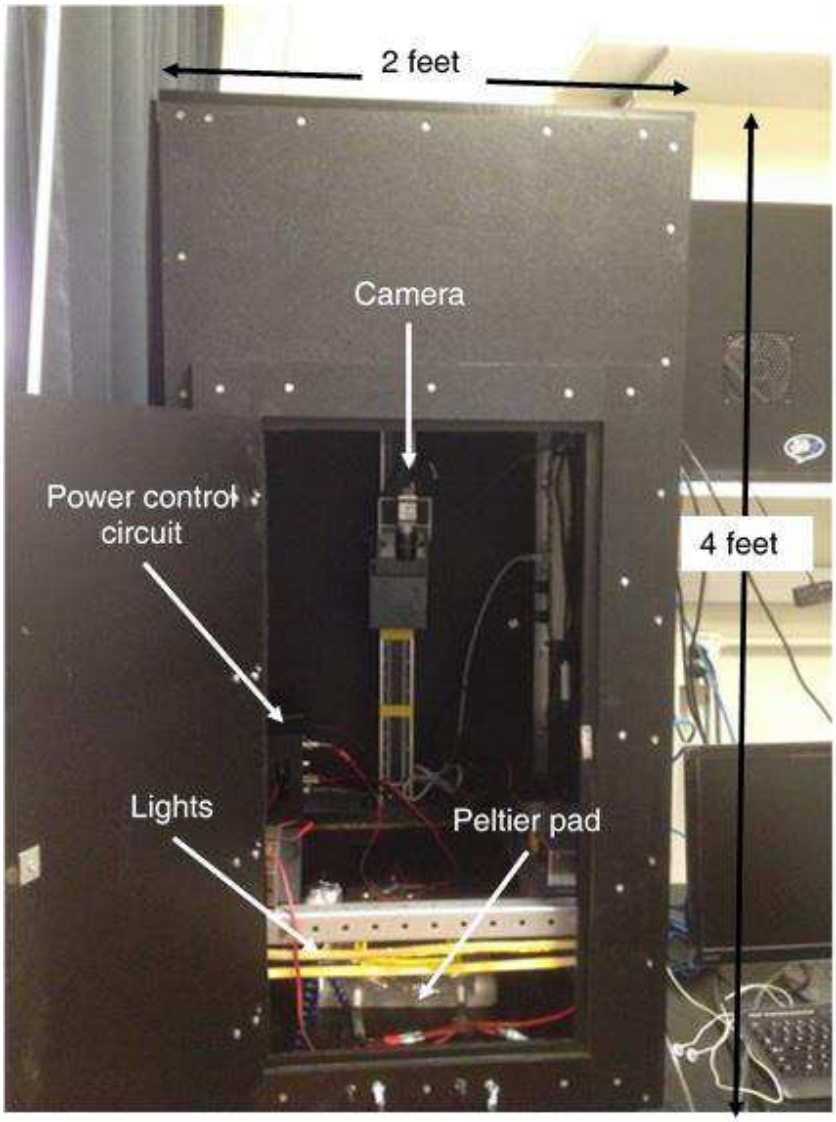

Supplementary Figure 11. Apparatus for assaying larval thermal nociception behavior. The black, plastic outer box (2' x 2' x 4') eliminates external light. We used red (560 nm) LED lights to evenly illuminate the larvae placed on the agarose plate. The camera we used to monitor the larval behaviors was a 2592 x 1944 Monochrome CMOS Camera (GigE). We used a TC-36-25-RS232 temperature controller (TE Technology) to control the temperature changes of the 12" x 12" Peltier plates. We integrated the controller program with the larval tracking software.

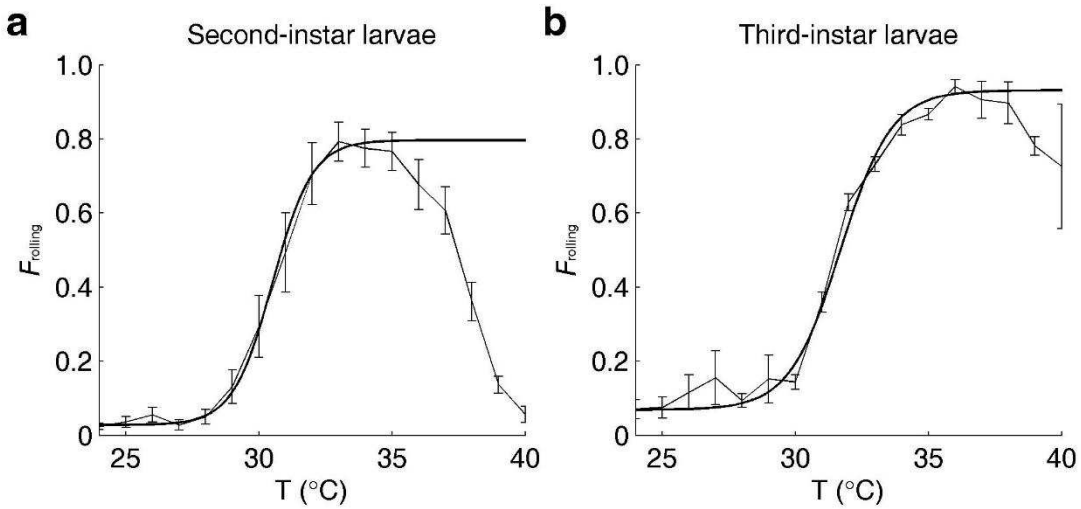

Supplementary Figure 12. Comparison of the rolling behaviors of control (w^{1118}) larvae at the indicated developmental stages (dT/dt = 0.2 °C/s). (**a**) Second-instar larvae (n = 7; ≥ 30 larvae per experiment). (**b**) Third-instar larvae (n = 3; ≥ 30 larvae per experiment).

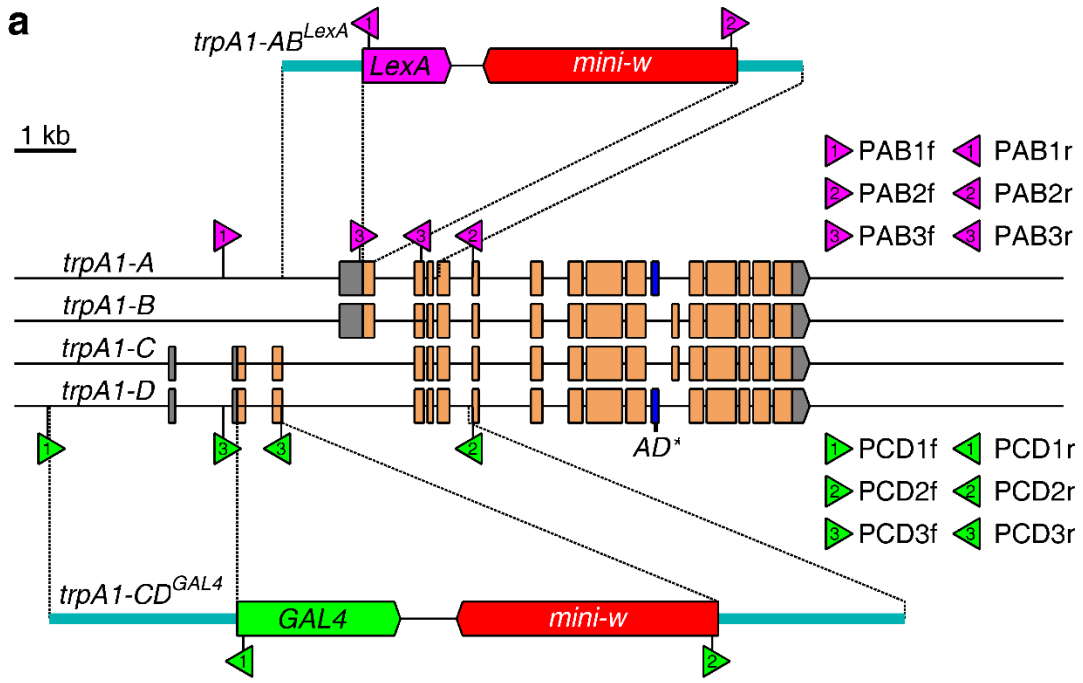

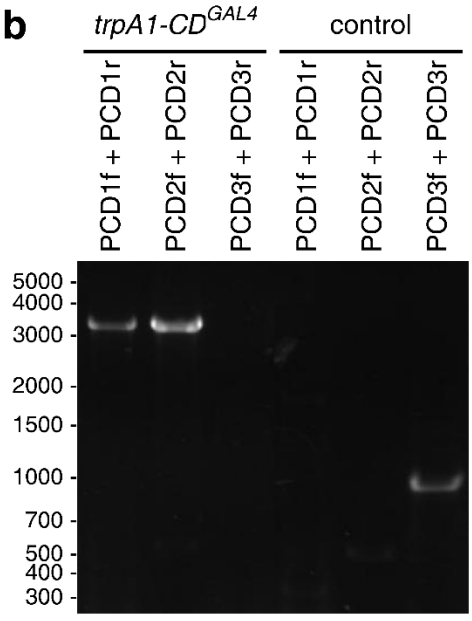

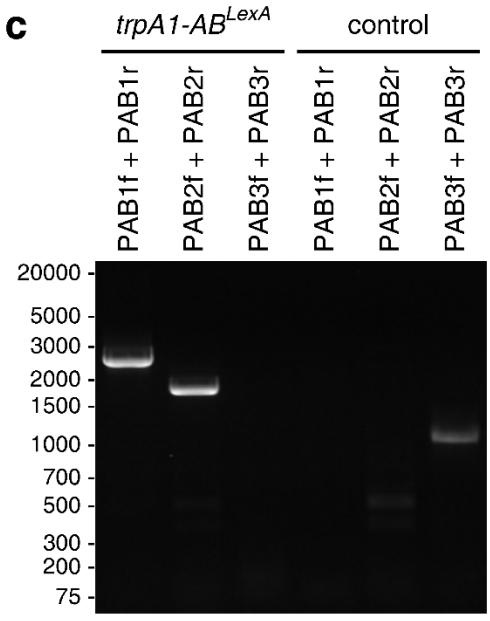

d

control TTGATGAGAAAACCGGAGAGTCGATTACGACCGCCAGTCCCATTCCGTTGC

trpA1-ACD^GAL4 TTGATGAGAAAACCGGA--GTCGATTACGACCGCCAGTCCCATTCCGTTGC

Supplementary Figure 13. Generation of the *trpA1* alleles. (**a**) The *trpA1-AB*^{LexA} allele was generated using the CRISPR/Cas9 system, and *trpA1-CD*^{GAL4} was generated by ends-out homologous recombination. The cyan bars indicate the homologous arms in the constructs used to generate the knockouts. The purple, green and red polygons represent the *LexA*, *GAL4* and *mini-w* genes, respectively, which were knocked into the genome. The gray and orange rectangles indicate the UTRs and *trpA1* coding sequences, respectively. The purple and green triangles represent the primer pairs used to identify the *trpA1-AB*^{LexA} and *trpA1-CD*^{GAL4} alleles, respectively. (**b**) Identification of *trpA1-CD*^{GAL4} by PCR analysis using the indicated primer pairs. (**c**) The identification of *trpA1-AB*^{LexA} by PCR analysis using the indicated primer pairs. (**d**) The sequences encompassing the mutation in the *trpA1-ACD*^{GAL4} allele. The dashes indicate the two base pairs deleted in *trpA1-ACD*^{GAL4}.

References

1. Gershow, M., et al., *Controlling airborne cues to study small animal navigation.* Nat. Methods, 2012. **9**(3): p. 290-6.
2. Mitchell, T.M., *Machine Learning* 1997: McGraw-Hill.
3. Manning, C.D., P. Raghavan, and H. Schütze, *Introduction to information retrieval*. 2008, Cambridge: Cambridge University Press.
4. Viswanath, V., et al., *Opposite thermosensor in fruitfly and mouse.* Nature, 2003. **423**(6942): p. 822-823.
5. Tracey, W.D., et al., *painless, a Drosophila gene essential for nociception.* Cell, 2003. **113**: p. 261-273.
6. Lee, Y., et al., *Pyrexia is a new thermal transient receptor potential channel endowing tolerance to high temperatures in Drosophila melanogaster.* Nat. Genet., 2005. **37**(3): p. 305-10.
7. Sokabe, T., et al., *Drosophila Painless is a Ca^{2+}-requiring channel activated by noxious heat.* J. Neurosci., 2008. **28**(40): p. 9929-9938.
8. Neely, G.G., et al., *TrpA1 Regulates Thermal Nociception in Drosophila.* PLoS One, 2011. **6**(8): p. e24343.
9. Zhong, L., et al., *Thermosensory and non-thermosensory isoforms of Drosophila melanogaster TRPA1 reveal heat sensor domains of a thermoTRP channel.* Cell Rep., 2012. **1**(1): p. 43-55.
10. Babcock, D.T., et al., *Hedgehog signaling regulates nociceptive sensitization.* Curr. Biol., 2011. **21**(18): p. 1525-33.

11. Oswald, M., et al., *A novel thermosensitive escape behavior in Drosophila larvae.* Fly (Austin), 2011. **5**(4).

12. Ni, L., et al., *A gustatory receptor paralogue controls rapid warmth avoidance in Drosophila.* Nature, 2013. **500**(7464): p. 580-4.

13. Kwon, Y., et al., *Control of thermotactic behavior via coupling of a TRP channel to a phospholipase C signaling cascade.* Nat. Neurosci., 2008. **11**: p. 871-873.

14. Kang, K., et al., *Modulation of TRPA1 thermal sensitivity enables sensory discrimination in Drosophila.* Nature, 2012. **481**(7379): p. 76-80.

15. Kim, S.H., et al., *Drosophila TRPA1 channel mediates chemical avoidance in gustatory receptor neurons.* Proc. Natl. Acad. Sci. USA, 2010. **107**: p. 8440–8445.

16. Kondo, S. and R. Ueda, *Highly improved gene targeting by germline-specific Cas9 expression in Drosophila.* Genetics, 2013. **195**(3): p. 715-21.

17. Yu, Z., et al., *Highly efficient genome modifications mediated by CRISPR/Cas9 in Drosophila.* Genetics, 2013. **195**(1): p. 289-91.

18. Gratz, S.J., et al., *Genome engineering of Drosophila with the CRISPR RNA-guided Cas9 nuclease.* Genetics, 2013. **194**(4): p. 1029-35.

19. Bassett, A.R., et al., *Highly efficient targeted mutagenesis of Drosophila with the CRISPR/Cas9 system.* Cell Rep., 2013. **4**(1): p. 220-8.

20. Klapoetke, N.C., et al., *Independent optical excitation of distinct neural populations.* Nat. Methods, 2014. **11**(3): p. 338-46.

21. Gordon, M.D. and K. Scott, *Motor control in a Drosophila taste circuit.* Neuron, 2009. **61**(3): p. 373-384.

22. Chen, T.W., et al., *Ultrasensitive fluorescent proteins for imaging neuronal activity.* Nature, 2013. **499**(7458): p. 295-300.

23. Wang, Y.Y., et al., *The nociceptor ion channel TRPA1 is potentiated and inactivated by permeating calcium ions.* J. Biol. Chem., 2008. **283**(47): p. 32691-703.

24. Jordt, S.E., et al., *Mustard oils and cannabinoids excite sensory nerve fibres through the TRP channel ANKTM1.* Nature, 2004. **427**(6971): p. 260-265.

25. Nagata, K., et al., *Nociceptor and hair cell transducer properties of TRPA1, a channel for pain and hearing.* J. Neurosci., 2005. **25**(16): p. 4052-61.

26. Zurborg, S., et al., *Direct activation of the ion channel TRPA1 by Ca^{2+}*. Nat. Neurosci., 2007. **10**(3): p. 277-9.

27. Stoney, S.D., Jr. and X. Machne, *Mechanisms of accommodation in different types of frog neurons.* J. Gen. Physiol., 1969. **53**(2): p. 248-62.

28. Hamada, F.N., et al., *An internal thermal sensor controlling temperature preference in Drosophila.* Nature, 2008. **454**(7201): p. 217-220.

29. Kwon, Y., et al., *Drosophila TRPA1 channel is required to avoid the naturally occurring insect repellent citronellal.* Curr. Biol., 2010. **20**(18): p. 1672-1678.

30. Bellen, H.J., et al., *The BDGP gene disruption project: single transposon insertions associated with 40% of Drosophila genes.* Genetics, 2004. **167**(2): p. 761-781.

31. Zhong, L., R.Y. Hwang, and W.D. Tracey, *Pickpocket is a DEG/ENaC protein required for mechanical nociception in Drosophila larvae.* Curr. Biol., 2010. **20**(5): p. 429-34.

32. Baines, R.A., et al., *Altered electrical properties in Drosophila neurons developing without synaptic transmission.* J. Neurosci., 2001. **21**(5): p. 1523-1531.

33. Berni, J., et al., *Autonomous circuitry for substrate exploration in freely moving Drosophila larvae.* Curr. Biol., 2012. **22**(20): p. 1861-70.

34. Shearin, H.K., et al., *Hexameric GFP and mCherry reporters for the Drosophila GAL4, Q, and LexA transcription systems.* Genetics, 2014. **196**(4): p. 951-60.

35. Duffy, J.B., D.A. Harrison, and N. Perrimon, *Identifying loci required for follicular patterning using directed mosaics.* Development, 1998. **125**(12): p. 2263-71.

36. Inagaki, H.K., et al., *Optogenetic control of Drosophila using a red-shifted channelrhodopsin reveals experience-dependent influences on courtship.* Nat. Methods, 2014. **11**(3): p. 325-32.

37. Taghert, P.H., et al., *Multiple amidated neuropeptides are required for normal circadian locomotor rhythms in Drosophila.* J. Neurosci., 2001. **21**(17): p. 6673-86.

38. Pfeiffer, B.D., et al., *Tools for neuroanatomy and neurogenetics in Drosophila.* Proc. Natl. Acad. Sci. USA, 2008. **105**(28): p. 9715-20.

39. Ni, J.Q., et al., *A Drosophila resource of transgenic RNAi lines for neurogenetics.* Genetics, 2009. **182**(4): p. 1089-1100.

40. Ohyama, T., et al., *High-throughput analysis of stimulus-evoked behaviors in Drosophila larva reveals multiple modality-specific escape strategies.* PLoS One, 2013. **8**(8): p. e71706.

41. Ben-lalli, A., et al., *Modeling heat transfer for disinfestation and control of insects (larvae and eggs) in date fruits.* J. Food Eng., 2013. **116**: p. 505-514.

42. Gong, W.J. and K.G. Golic, *Ends-out, or replacement, gene targeting in Drosophila.* Proc. Natl. Acad. Sci. USA, 2003. **100**(5): p. 2556-61.

43. Moon, S.J., et al., *A Drosophila gustatory receptor essential for aversive taste and inhibiting male-to-male courtship.* Curr. Biol., 2009. **19**: p. 1623-1627.

44. DeCoursey, T.E. and V.V. Cherny, *Temperature dependence of voltage-gated H^+ currents in human neutrophils, rat alveolar epithelial cells, and mammalian phagocytes.* J. Gen. Physiol., 1998. **112**(4): p. 503-22.

45. Klein, M., et al., *Sensory determinants of behavioral dynamics in Drosophila thermotaxis.* Proc. Natl. Acad. Sci. USA, 2015. **112**(2): p. E220-9.

46. Ohyama, T., et al., *A multilevel multimodal circuit enhances action selection in Drosophila.* Nature, 2015. **520**(7549): p. 633-9.

47. Gracheva, E.O., et al., *Molecular basis of infrared detection by snakes.* Nature, 2010. **464**(7291): p. 1006-11.

Curriculum Vitae

CURRICULUM VITAE FOR Ph.D. CANDIDATES

The Johns Hopkins University School of Medicine

JUNJIE LUO 06/09/2017

Education

Ph.D. (expected)	2017	Biological Chemistry Mentor: Craig Montell Ph.D.	Johns Hopkins School of Medicine
B.S.	2008	Biological Science and Technology	Tsinghua University

Other Professional Experience

Research rotation 2010 Takanari Inoue Lab, Johns Hopkins School of Medicine

Research rotation 2010 Craig Montell Lab, Johns Hopkins School of Medicine

Research rotation 2009 Richard Huganir Lab, Johns Hopkins School of Medicine

Academic and other honors

2008	Bronze Medal International Genetically Engineered Machine (iGEM) Foundation	
2007	Excellent Student Scholarship	Tsinghua University
2007	Second Prize in Challenge Cup	Tsinghua University
2006	Scholarship for Academic Excellence	Tsinghua University
2005	Excellent Student Scholarship	Tsinghua University
2003	Second Prize China Physics Olympiad (CPhO)	

Publications, peer reviewed

Xu C, **Luo J**, He L, Montell C, Perrimon N. (2017) Oxidative stress induces stem cell proliferation via TRPA1/RyR-mediated Ca2+ signaling in the Drosophila midgut ***eLife***. 6.

Luo J, Shen WL, Montell C. (2017) TRPA1 mediates sensation of the rate of temperature change in Drosophila larvae. ***Nature Neuroscience.*** **20**: 34-41.

Sokabe T, Chen HC, **Luo J**, montell C. (2016) A switch in thermal preference in Drosophila larvae depends on multiple rhodopsins. ***Cell Reports.*** **17**: 336-344.

Huang J, Liu W, Qi Y, **Luo J**, Montell C. (2016) Neuromodulation of Courtship Drive through Tyramine-Responsive Neurons in the Drosophila Brain. ***Current Biology.*** **26** (17): 2246-2256.

Cai D, Dai W, Prasad M, **Luo J**, Gov NS, Montell DJ. (2016) Modeling and analysis of collective cell migration in an in vivo three-dimensional environment. ***Proceedings of the National Academy of Sciences.*** **113** (15): E2134-E2141.

Hussain NK, Thomas GM, **Luo J**, Huganir RL. (2015) Regulation of AMPA receptor subunit GluA1 surface expression by PAK3 phosphorylation. ***Proceedings of the National Academy of Sciences.*** **112** (43): E5883-E5890.

Wu H, **Luo J**, Yu H, Rattner A, Mo A, Wang Y, Smallwood PM, Erlanger B, Wheelan SJ, Nathans J. (2014) Cellular resolution maps of x chromosome inactivation: implications for neural development, function, and disease. ***Neuron***. 81(1): 103-119.

Shen WL, Kwon Y, Adegbola AA, **Luo J**, Chess A, Montell C. (2011) Function of rhodopsin in temperature discrimination in Drosophila. ***Science.*** **331** (6022): 1333-1336.

Luo J, Wang J, Ma TM, Sun Z. (2010) Reverse engineering of bacterial chemotaxis pathway via frequency domain analysis. ***PLoS One.*** **5** (3): e9182.

Sun Z, Luo J, Zhou Y, **Luo J**, Liu K, Li W. (2009) Exploring phenotype-associated modules in an oral cavity tumor using an integrated framework. ***Bioinformatics.*** **25**(6): 795-800.

Luo S, Zhang B, Dong XP, Tao Y, Ting A, Zhou Z, Meixiong J, **Luo J**, Chiu FC, Xiong WC, Mei L. (2008) HSP90 beta regulates rapsyn turnover and subsequent AChR cluster formation and maintenance. ***Neuron.*** **60**(1): 97-110.

Publications, chapters and non-peer reviewed

Venkatachalam K, **Luo J**, Montell C. (2014) Evolutionarily conserved, multitasking TRP channels: lessons from worms and flies. ***Mammalian Transient Receptor Potential (TRP) Cation Channels, Handb Exp Pharmacol.*** **223:** 937-962.

Posters

Junjie Luo, Shen WL, Montell C. A Mechanism for Detecting the Rate of Temperature Change in Drosophila. ***Biophysical Journal,*** 2015; **108** (2): 123a.

Junjie Luo. A Dynamic Model Utilizing Linear Operators for the Characterization of Stochastic Gene Expression. ***Biophysical Journal,*** 2013; **104** (2): 494a.